1

INTRODUCTION

John Thornton and Kao-Cheng Huang

The topic of lens antennas was widely investigated during the early development of microwave antennas and was influenced by the extensive body of existing work from optics. Subsequently, interest declined somewhat as lens antennas were overtaken by reflectors for high efficiency, large aperture antennas; and by arrays for shaped-beam, multi-beam, and scanning antennas. Quite recently, as research interest has expanded into the use of millimeter wave and sub-millimeter wave frequency bands, lens antennas have again attracted developers' attention.

This chapter is organized as nine sections to introduce the basics of lens antennas. Section 1.1 gives an overview of lens antennas, including its advantages, disadvantages, and the materials encountered. This is followed by a discussion of antenna feeds at Section 1.2. Then Section 1.3 introduces the fundamentals of the Luneburg lens (a topic to which Chapters 6 and 7 are dedicated). Section 1.4 introduces quasi-optics and Section 1.5 treats design rules. A discussion of metamaterials for lens antennas makes up Section 1.6 and then the planar lens array, which is a relative of the reflect-array antenna, follows in Section 1.7. Applications are proposed in Section 1.8 and measurement techniques and anechoic chambers discussed in the final section.

Modern Lens Antennas for Communications Engineering, First Edition. John Thornton and Kao-Cheng Huang.

1.1 LENS ANTENNAS: AN OVERVIEW

The use of dielectric lenses in microwave applications seems to date back to the early days of experiments associated with the verification of the optical properties of electromagnetic waves at 60 GHz [1]. However, it was not until World War II that lenses gained interest as antenna elements. Even then they were not widely used because of their bulky size at rather low frequencies.

Nowadays there is a renewed interest in dielectric lenses, not least because of the rapidly growing number of applications for millimeter waves where lens physical dimensions have acceptable sizes. Besides, very low loss dielectric materials are available, and present-day numerically controlled machines enable low-cost fabrication of quite sophisticated lenses made with very good tolerances.

In one of the earliest dielectric lens antenna applications, a homogeneous lens was designed to produce a wide-angle scanning lobe [2]. Also, homogeneous lenses have been used as phase front correctors for horns. The lens is often mounted as a cap on a hollow metallic horn [3]. In this configuration the lens surfaces on both sides can be used to design for two simultaneous conditions. In addition, lenses may be designed to further control the taper of the field distribution at the lens aperture [4] or to shape the amplitude of the output beam in special applications [5].

The aperture of a solid dielectric horn can be shaped into a lens to modify or improve some radiation characteristics [6]. For instance, the aperture efficiency of a solid dielectric horn may be improved by correcting the aperture phase error. Alternatively we may use a lens to shape the amplitude of the output beam or to improve the cross-polarization performance, but because there is only the one lens surface to be varied, only one of these design targets might be made optimum.

1.1.1 The Microwave Lens

In optics, a lens refracts light while a mirror reflects light. Concave mirrors cause light to reflect and create a focal point. In contrast, lenses work the opposite way: convex lenses focus the light by refraction. When light hits a convex lens, this results in focusing since the light is all refracted toward a line running through the center of the lens (i.e., the optical axis). Save for this difference, convex lens antennas work in an analogous fashion to concave reflector antennas. All rays between wavefronts (or phase fronts) have equal optical path lengths when traveling through a lens. Fresnel's equations, which are based on Snell's law with some additional polarization effects, can be applied to the lens surfaces.

In general, lenses collimate incident divergent energy to prevent it from spreading in undesired directions. On the other hand, lenses collimate a spherical or cylindrical wavefront produced respectively by a point or line source feed into an outgoing planar or linear wavefront. In practice, however, complex feeds or a multiplicity of feeds can be accommodated since performance does not deteriorate too rapidly with small off-axis feed displacement.

There are two main design concepts used to reach different goals.

1. Conventional (e.g., hyperbolical, bi-hyperbolical, elliptical, hemispherical) or shaped lens antennas are used simply for collimating the energy radiated from a feed.
2. In the case of shaped designs, more complex surfaces are chosen for shaping the beam to produce a required radiation pattern, or for cylindrical and spherical lenses for beam scanning with either single or multiple feeds.

Lenses can also be placed into one or other of the categories of slow wave and fast wave lenses (Fig. 1.1). The terms relate to the phase velocity in the lens medium. The slow-wave lens type is illustrated in Figure 1.1a. Here, the electrical path length is increased by the medium of the lens, hence the wave is retarded.

The most common type is the dielectric lens but another example is the *H*-plane metal-plate lens (Fig. 1.2). (The *H*-plane is that containing the magnetic field vector

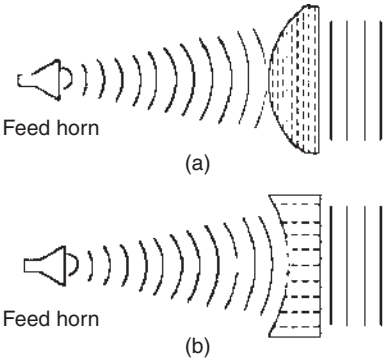

Figure 1.1. Comparison of (a) slow-wave or dielectric lens and (b) *E*-plane metal-plate (fast-wave) lens types. Wave fronts are delayed by (a) but advanced by (b).

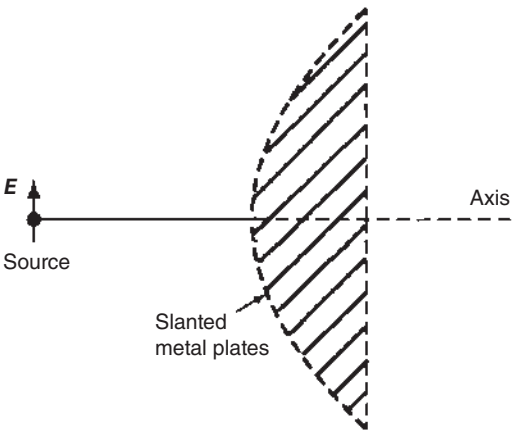

Figure 1.2. *H*-plane metal plate lens antenna.

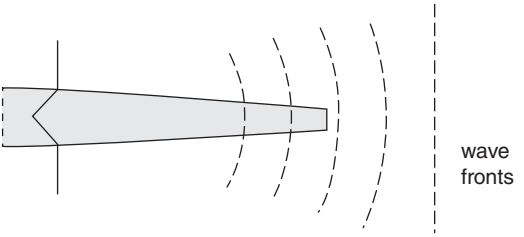

Figure 1.3. A form of basic lens antenna: the polyrod.

and the also the direction of maximum radiation, or main lobe boresight. The magnetizing field or *H*-plane lies at a right angle to the electric or *E*-plane.)

Figure 1.1b shows the fast-wave lens type where the electrical path length is effectively made shorter by the lens medium, so the wave is advanced. *E*-plane metal-plate lenses are of the fast-wave type. (The *E*-plane is that containing the electric field vector and also the direction of maximum radiation. The *E*-plane and *H*-plane are orthogonal to each other and determine the polarization sense of a radio wave.)

In terms of materials, dielectric lenses may be divided into two distinct types:

1. Lenses made of conventional dielectrics, such as Lucite® or polystyrene.
2. Lenses made of artificial dielectrics such as those loaded by ceramic or metallic particles.

Lens antennas tend to be directive rather than omnidirectional i.e. they usually exhibit a single, distinct radiation lobe in one direction. In this case, they might be thought of as "end-fire" radiators. With this in mind, a dielectric rod, as shown in Figure 1.3, is a good example. Because the rod is usually made from polystyrene, it is called a *polyrod*. A polyrod acts as a kind of imperfect or leaky waveguide for electromagnetic waves. As energy leaks from the surface of the rod it is manifested as radiation. This tendency to radiate is deliberate, and the rod's dimensions and shape are tailored to control the radiation properties which are discussed in proper detail in Chapter 3.

In contrast to polyrod antennas, most lens dimensions are much larger than the wavelength, and design is based on the quasi optics (QO) computations. Snell's refraction law and a path length condition (or eventually an energy conservation condition) are then used to define the lens surface in the limit as the wavelength tends to zero. Depending on the lens shape, diffraction effects may give rise to discrepancies in the final pattern. While these comments really concern axis-symmetric lenses, on the other hand, literature on arbitrary shaped dielectric lenses and three-dimensional amplitude shaping dielectric lens is also available [5].

1.1.2 Advantages of Lens Antennas

Lenses are an effective antenna solution where beam shaping, sidelobe suppression, and beam agility (or steering in space) can be achieved simultaneously from a compact

assembly. Dielectric lenses may also bring about these system advantages economically because they can be manufactured through molding or automated machining in reasonably high quantities, and these processes offer suitable tolerances. Lenses are used to convert spherical phase fronts into planar phase fronts across an aperture to enhance its directivity much like parabolic reflectors. For this purpose lenses present an advantage over reflectors in that the feed is located behind the lens, thus eliminating aperture blockage by the feed and supporting struts, with no need for offset solutions. This ability to illuminate the secondary aperture (lens vs. reflector) in a highly symmetric fashion but without aperture blockage leads to the benefit that lens antennas can have low distortions and cross-polarization.

Microwave lenses are of course not without disadvantages and among these are dielectric losses and reflection mismatch. A mitigation against loss of course is to use low loss materials, such as Teflon, polyethylene, and quartz, where material loss can be reduced to quite negligible levels. Solutions for reflection mismatch include the use a quarter wavelength anti reflection (AR) layer, or "coating" if such a layer can be said to be thin. To follow up here with some examples, alumina-loaded epoxy has been used with good results as an anti-reflection coating for silicon lenses [7]. However, the epoxy material suffers from large absorption loss above 1 THz [8]. Englert et al. [9] has successfully coated both sides of a silicon window with 20 μm of low-density polyethylene (LDPE, $n \sim 1.52$) to achieve anti-reflection (AR) performance at $\lambda = 118\,\mu m$. Other common plastics such as *Mylar* and *Kapton* are potential candidates because their refractive indices are close to the required value of $(n_{silicon})^{0.5} \sim 1.85$ [10]; however, such materials may be difficult to apply to a small silicon lens. Thin films of parylene can be used as an AR layer for silicon optics and show low-loss behavior well above 1 THz [10]. In contrast, at lower frequencies, for example, 10 to 60 GHz, air grooves may be machined into a lens surface to yield an effective air-dielectric composite layer of intermediate index—such a fabrication technique is encountered in commercially available lens antennas. This is also said to reduce gain variation with frequency.

1.1.3 Materials for Lenses

Real-life antennas make use of real conductors and dielectrics. It is thus useful to recall some of their characteristics. A conductor is defined as a material with a large number of free detachable electrons or a material having high conductivity. Typical conductors used in antennas are

- Silver (conductivity = 6.14×10^7/ohm/m)
- Copper (conductivity = 5.8×10^7/ohm/m)
- Aluminum (conductivity = 3.54×10^7/ohm/m)

A dielectric is essentially an insulator: a material with few free detachable electrons or with a low value of conductivity. In many cases conductivity for a good conductor may be taken as infinity and for a good dielectric as zero.

To produce lens antennas, it is necessary to select a material which is mechanically and electromagnetically stable. A typical choice of material could be based on a relative

permittivity ranging from about 1.2 to 13—indeed these materials are either in use today or are expected to be used for millimeter wave antenna systems. Because of time and space considerations, not all materials available today will be compared here, but it is felt that these examples are representative and other common substrate materials have properties roughly within the range of those considered here.

The dielectric loss factor is also known as the dissipation factor. It is defined from the tangent of the loss angle ($tan\,\delta$), and is hence also called the loss tangent. Put another way, the loss angle is that whose tangent is derived from the ratio of the imaginary to the real part of the dielectric permittivity: Im (ε)/Re (ε).

Thus we are quantifying the ratio of the resistive (also lossy, and imaginary) and the reactive (also lossless, and real) components of the dielectric constant. For low loss materials the former term should be very small. The dielectric constant (ε) and loss tangent ($tan\,\delta$) can be difficult to measure accurately at microwave frequencies. Often, techniques are used which look at the properties of resonators and might compare their behavior with and without the insertion of a sample of dielectric material. Vector network analyzer would typically be used. Some typical values are identified in Table 1.1.

1.1.4 Synthesis

Synthesis of lenses has received plenty of attention, though perhaps less so than reflector antennas or other types. Spherical lenses (Fig. 1.4) present a good example of how synthesis and optimization can be applied. The topic will be covered in more detail in Chapters 6 and 7, but for present section it is worth pointing out that the ideal spherical lens configuration—the Luneburg lens—is exceedingly difficult to construct according to the strict formulation. When approximations are applied, by using discrete dielectric layers for example, compromises must be sought. These trade the antenna efficiency against the number of layers and hence difficulty of construction [12]. Modern computers assist greatly with the study of these effects. Computer optimization routines are widely applied in electromagnetics and microwave engineering. Different niche approaches have advantages and disadvantages depending on their precise area of application. In Reference 12 genetic algorithms were reported to have had powerful effect in optimizing the desired lens gain and sidelobe suppression, where the optimizer variables were the dielectric constant and radial width of each lens layer.

Komljenovic et al. [13] pointed out that of the many global optimization techniques available, those used most extensively so far in electromagnetics have been relatively few. These have been:

- genetic algorithms,
- particle swarm optimization.
- the multidimensional conjugate gradient method.

The genetic algorithm (GA), as a class of optimization kernel, has been applied widely and with success to many problems [14] in addition to the spherical lens we have already briefly mentioned. The GA approach is also know of as evolutionary computation, or is sometimes synonymous with the general class of evolutionary algorithms

TABLE 1.1. Electrical Properties of Microwave Substrates [11]

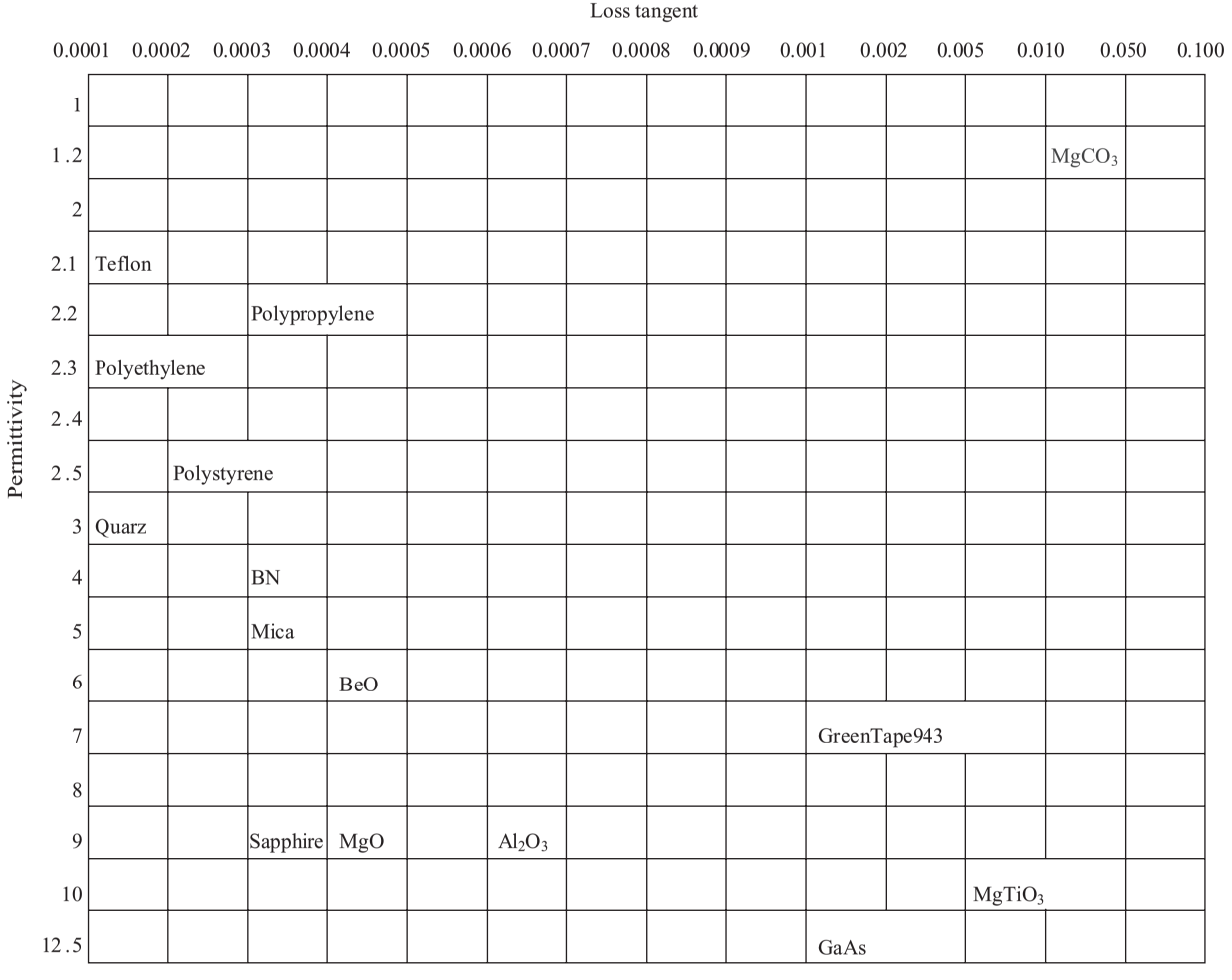

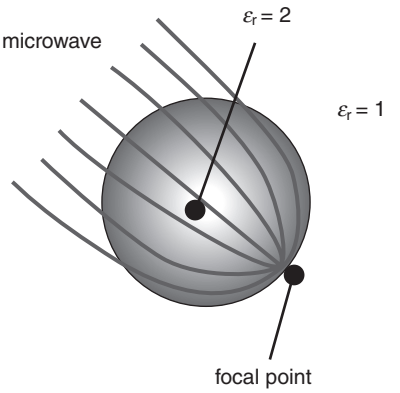

Figure 1.4. An example of a spherical stepped-index lens.

inspired by biological processes. In this context, we encounter such mechanisms as selection, mutation and inheritance, and the health of populations and so on.

A more recent technique, also under the "evolutionary algorithm" banner, is called "particle swarm" optimization [15]. This is based on models for the intelligence and movement of individuals in swarms and has been applied successfully to problems in electromagnetics. At first, relatively small numbers of individual states, perhaps fewer than 30, were considered adequate to model swarms. More recently though, and for more exhaustive optimization, larger numbers than this have been recommended, for example, in Reference 13, where the technique was applied to cylindrical lenses. Unsurprisingly, the computational load should be expected to increase as optimization techniques become ever more complex. Fortunately, computer performance is ever advancing.

On a final note for this section, a multidimensional conjugate gradient method has also been used for the successful optimization of some quite complicated shaped lens designs which have also had arbitrary geometries [16]. Again, the technique is iterative.

1.2 FEEDS FOR LENS ANTENNAS

The feeding methods of lens antennas can be any other type of antenna: horns, dipoles, microstrip (e.g., patch), and even arrays of antenna elements.

In practice horns (or just open ended waveguides) and patches are most commonly used, or, in some cases, arrays of such elements.

1.2.1 Microstrip Feeds

The most often cited advantages of microstrip (or "patch") antennas include their low mass, ease and low cost of fabrication, robustness, and ease of integration with other microwave printed circuits and connections. They are typically also low profile,

occupying either just the thickness of the printed circuit, or the laminate plus a low dielectric constant spacing layer, which might just be air. The latter approach tends to increase the bandwidth of what is otherwise a narrow-band radiator [17].

As a primary feed for a lens antenna, the properties of patch antennas are useful in some cases but not in others. For example, where a patch antenna is used to illuminate a hemispherical lens-reflector, which is a type of reduced height scanning antenna, the low profile of the patch can help to avoid the headroom encroachment that would be caused by a waveguide or horn type feed. However, disadvantages of the patch include ohmic loss in both the metallization layer and the substrate, which can increase dramatically with frequency.

Many single-patch geometries can be used, for example, rectangular, circular, bow-tie, planar-conical, and so on. Where these can be combined in array configurations there is more scope to select or optimize the pattern which illuminates the so-called secondary aperture (the lens).

In Chapter 4 we will show some design examples of types of lens integrated directly onto patch antenna substrates.

1.2.2 Horn Feeds

In contrast to the narrow-band and low-efficiency printed circuit antenna discussed above, the waveguide or horn type tends to be both much more wide-band and more efficient. These advantages tend to accrue at the cost of physical volume, mass, and to some extent fabrication expense compared to patches at least. Considering that dielectric lenses (i.e., not zoned for reduced thickness) are very wide band in operation it can make sense to use them with a similarly wide-band primary feed. The horn's bandwidth is, to a first order at least, determined by that of the feeding waveguide and this will exhibit a cut-off behavior at the lower threshold and higher order mode propagation at a higher threshold. Used as a primary feed for a lens, the horn is carrying out a very similar function as when used with a reflector, but with the lens the horn will not introduce aperture blockage. In Chapter 5 we will present a low sidelobe lens antenna where this property is exploited.

Due to the lower propagation velocity, phase errors at the plane aperture of a solid dielectric horn are higher than for a conventional metallic horn of comparable size, thus placing a lower limit to the maximum achievable gain. Following a standard approach for high-performance metallic horns, where a dielectric lens is positioned at the horn aperture in order to correct the phase error, the dielectric horn aperture may be shaped into a lens [18].

Here, a practical engineering tip is that the feed should provide an illumination of the antenna edge at the level of −10 dB with respect to the central point. Then, the antenna performance in terms of directive gain is optimal. This empirical rule is approximately valid for any QO system, although for systems carrying out extensive manipulations of Gaussian beams a more conservative rule of −20 dB to −35 dB is common [19].

There are other applications where the design is not necessarily to maximize antenna gain, but rather to shape the beam. Again, a lens may be used to modify the

basic horn radiation pattern. A particular design goal is discussed in detail in Chapter 5 where the case study is for a low sidelobe elliptic beam antenna for mm-wave communications.

Intrinsic to the dielectric horn-lens geometry, there is only one refracting surface and so amplitude shaping and phase correction conditions can not be imposed simultaneously. The situation is different for metallic horns where correction lenses have two refracting surfaces, one on the horn side and the other on the output (free space) side, enabling two independent conditions to be met. In this case, however, rather than designing the second refracting surface for an amplitude condition it is often better to set the input surface as planar and to design the output surface according to the path length condition, since an appropriate choice of permittivity leads to convenient field distribution on the aperture [18].

Another design approach can be to employ moderate loss materials to reduce the field amplitude toward the lens axis where its depth increases, thus reducing the field taper across the aperture without interfering with the other lens surface [20] at the expense of gain.

Horn-lenses are just one possible application of dielectric lenses. Most commonly used are axis-symmetric lenses, designed as collimating devices possibly with more than one focal point for scanning and multibeam applications. In the simplest designs for single focus lenses one of the two lens surfaces is arbitrarily fixed to some preferred shape while phase correction condition defines the other surface. For scanning and multibeam applications the second surface is used to introduce a further condition to minimize aberrations originated by off-axis displacements of the feed position.

The main shortcoming of horns lies in their bulkiness that can make integration challenging. A less bulky alternative would be an open ended waveguide, but this would reduce optimization opportunities and in any case open ended waveguides could be found to be too cumbersome for integration in many cases.

Somewhat less work has been reported on dielectric lens designs incorporating amplitude shaping conditions. Here, the motivation is to produce a controlled field distribution over the lens aperture [21]. Routines to calculate two surface lenses for simultaneous phase and amplitude shaping are given in Reference 22. Another motivation is to shape the output beam into an hemispherical or a secant squared (sec^2) pattern for constant flux applications. A renewed interest in these type of patterns comes from emerging millimeter wave mobile broadband cellular systems and wireless local area network applications where non-symmetric lenses may be required [23].

Lens design, based on quasi optics, is addressed either for aperture phase error correction or for output beam shaping. For phase correction the formulation is restricted to circular-symmetric geometries, but methods can be adapted to suit pyramidal dielectric horns as well.

1.3 LUNEBURG AND SPHERICAL LENSES

Spherical lenses will be covered in much more detail in Chapters 6 and 7, along with some accounts of practical developments and applications pursued by the authors in

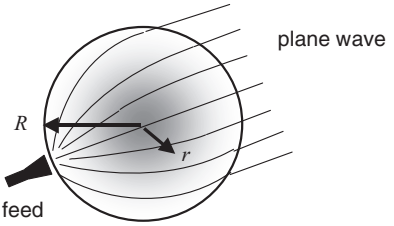

Figure 1.5. Ray paths in a Luneburg lens [24, 25].

the course of several research programs. For the current chapter, a short introduction is offered.

Unlike a paraboloid reflector, or a conventional focusing lens of one of the types introduced in the above paragraphs, a spherical lens does not exhibit a point focus. Rather, its symmetry gives rise to a focal region defined by a spherical surface which is concentric with the lens. Put another way, a feed may be placed at any position around the edge of the lens (or, in special cases, within the interior of the lens). A straightforward corollary of this symmetry is the ability to use several feeds, each giving rise to a separate beam which shares the lens aperture. Thus, a multi-beam antenna is readily offered. Similarly, a feed (or several feeds) mechanically scanned with respect to a spherical lens gives rise to a scanning antenna with very wide scan angle properties, and without scanning loss. A switched beam antenna may similarly be produced.

Where a spherical lens is constructed from a single, homogeneous dielectric material (a polymer e.g., Fig. 1.5) we have a "constant index lens." A disadvantage is that its collimating properties tend to be mediocre, particularly as electrical size increases. In an alternative approach, proposed by R. K. Luneburg in 1943 [24] the sphere is made of materials with non-constant refractive index, that is, where relative dielectric constant ε_r varies with the square of radius:

$$\varepsilon_r = 2 - (r/R)^2$$

where r is radius from the center point and R is outer radius of lens. This formulation gives rise to foci lying on the outer surface at $r = R$. Furthermore, the focus is at a single point in a manner analogous to any properly collimating device (dish, lens etc)—all of the aperture contributes and, given a suitable illumination, the aperture efficiency can be unity at least in theory. This property is irrespective of diameter, quite unlike a constant index lens where the efficiency will be less than unity and also decreases with increasing diameter.

Figure 1.5 illustrates the approximate ray paths for the Luneburg lens case and hence shows curved paths within the dielectric. Luneburg did not have the opportunity to implement such an antenna, as no suitable materials or manufacturing procedures were available at that time. Today, practical "Luneburg" lenses are made from sets of concentric dielectric layers, and as such are really approximations to the ideal case [25].

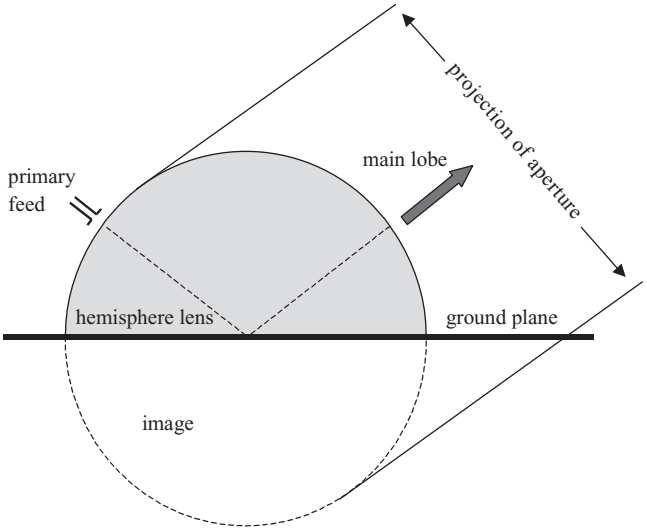

Figure 1.6. Hemisphere lens antenna.

A hemispherical lens antenna is also commonly used in conjunction with a reflective ground plane, the latter gives rise to an image of the hemisphere and so recovers the full aperture that would be presented by a sphere (Fig. 1.6). This arrangement offers mass and space reductions, and can be easier to mechanically stabilize. This might also be called a "lens-reflector" since the flat planar reflector is an integral part of the antenna aperture and contributes to its collimating properties. Of course, the extension of the reflector must be adequate to produce the required image of the hemisphere, and the necessary dimension is also a function of elevation angle (the feed angle with respect to the reflector plane). An inadequate reflector extension will introduce a reduction in effective aperture which amounts to a scanning loss. The topic is covered quite thoroughly in Chapter 7 where recent advances in practical antennas of this type are reported.

This configuration also offers a relatively low-profile solution, and this property makes the hemisphere antenna particularly attractive as a scanning antenna for applications where headroom is limited. The layout is illustrated in Figure 1.7, where it can be seen that the effective aperture height of the hemisphere with reflecting plane can be up to twice that of a conventional reflector antenna [25]. Again, recent practical developments are discussed in Chapter 7.

A variant of the spherical Luneburg lens is cylindrical and where the variation in dielectric constant occurs in just two dimensions rather than three. The "cylindrical Luneburg" lens is therefore somewhat less problematic to manufacture than its spherical parent, but it does offer beam collimation in just one axis, leading to a fan shaped beam rather than a pencil beam. Various approaches to realizing the required variation in dielectric constant, using a juxtaposition of two different materials, are presented in

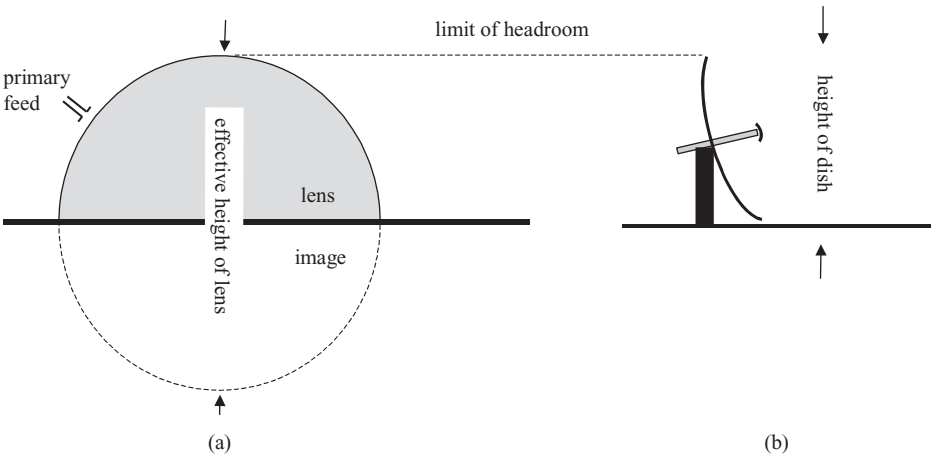

Figure 1.7. Comparison of (a) hemisphere plus plane reflector (b) conventional reflector antenna.

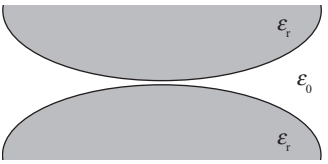

Figure 1.8. Cylindrical Luneburg lens formed from two dielectric discs [26].

Reference 26, along with experimental results. One such geometry is quite elegant because one of the materials is air and the other takes the form of a pair of machined polymer discs as illustrated in cross section in Figure 1.8.

In the 1970s, dielectric lenses were developed in Russia by several organizations [27]; these were mainly used in defense applications. Later, in the 1990s–2000s the Konkur company of Moscow were promoting Luneburg lenses of their own manufacture, although at the time of publication little evidence has been found to indicate that they are still active. Today the Luneburg lens is an attractive candidate antenna for multibeam wideband millimeter wavelength indoor and outdoor communication systems and for airborne surveillance radar applications. Manufacturers that appear to be still active are "Luntec" of France, and Rozendal Associates of Santee, California. Also, during the 2000s, Sumitomo Electric Industries of Japan were manufacturing lenses for multi-beam satellite TV, primarily in the receive only domestic market in Japan. (At the time of writing it is not known to the authors whether this continues although some anecdotal evidence suggests not. The brand "LuneQ" is still encountered in this context.)

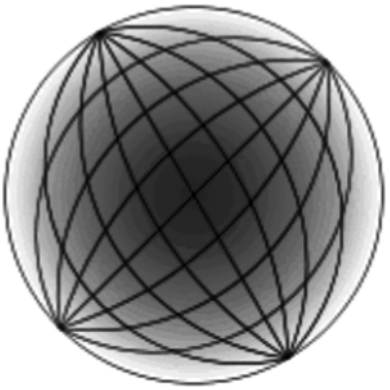

Figure 1.9. Maxwell's fish-eye lens, with dark color representing increasing refractive index.

1.4 QUASI OPTICS AND LENS ANTENNAS

Originally, quasi-optics (QO) applications of classical homogeneous lens designs remained restricted to aperture phase correction in millimeter wave horn feeds. At the same time, inhomogeneous lenses that were only theoretical curiosities at traditional optical wavelengths were realized in the microwave range and still attract much attention. These include the Luneburg lens, the Maxwell "fish-eye" lens (Fig. 1.9), and others. The spherical or cylindrical Luneburg lens (as we have seen) has a dielectric constant varying smoothly from 2 at its center to 1 at its outer boundary, which is the focal surface in the geometric optics (GO) approximation. While lens dimensions are larger than microwave wavelengths, spheres with a dielectric constant varying smoothly on the scale of the wavelength are almost impossible to fabricate. Therefore various sorts of Luneburg lenses which employ discrete dielectric layers have been devised. The oldest types consisted of a finite number of spherical or cylindrical layers each with constant permittivity.

Quasi optics can be considered to be a specific branch of microwave science and engineering [28–30]. The term "quasi optics" is used to characterize methods and tools devised for handling, both in theory and in practice, electromagnetic waves propagating in the form of directive beams, width w is greater than the wavelength λ, but which is smaller than the cross-section size, D, of the limiting apertures and guiding structures: $\lambda < w < D$.

Normally we have $D < 100\lambda$, and devices as small as $D = 3\lambda$ can be analyzed with some success using QO. Therefore QO phenomena and devices cannot be characterized with geometrical optics (GO) that requires $D > 1000\lambda$, and both diffraction and ray-like optical phenomena must be taken into account. It is also clear that, as Maxwell's equations (although not material equations) are scalable in terms of the ratio D/λ, the range of parameters satisfying the above definition sweeps across all the ranges of the electromagnetic spectrum, from radio waves to visible light (Fig. 1.10) and beyond.

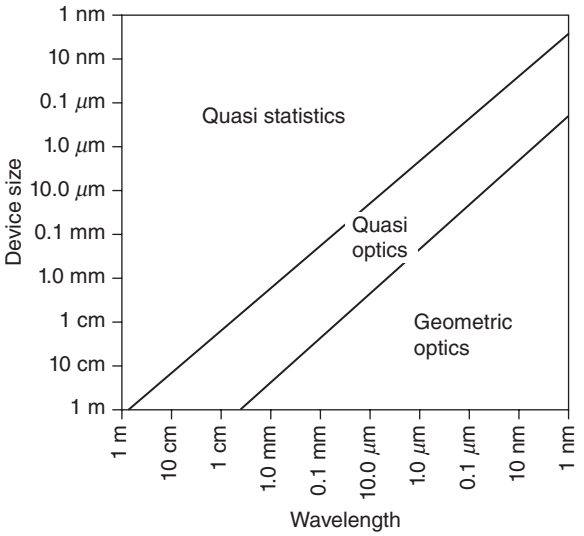

Figure 1.10. A diagram showing the place of quasioptical (QO) techniques with respect to geometrical optic (GO) and quasistatic techniques, in the plane of the two parameters-device size and wavelength.

Therefore QO effects, principles and devices can be encountered in any of these ranges, from skyscraper-high deep-space communication reflectors to micron-size lasers with oxide windows.

As a universal QO device, the dielectric lens was first borrowed from optics by O. Lodge for his experiments at a wavelength of 1 meter in 1889 [31], then used in microwave and millimeter wave systems in the 1950–1980s, and is today experiencing a third generation in terahertz receivers. Moreover, as the above relation among the device size, beam size, and wavelength is common in today's optoelectronics, it is clear that QO principles potentially may have a great impact on this field of science as well. Nevertheless, in the narrow sense, the term QO still relates well to the devices and systems working with millimeter and sub-millimeter waves. E. Karplus apparently coined the term quasi optics in 1931 [32], and then it was forgotten for exactly 30 years before being used again [33]. A parallel term *microwave optics* was used in several remarkable books and review articles of the 1950–1960s [34].

If compared with the classical optics of light, millimeter wave and sub- millimeter wave QO have several features. First, electromagnetic waves display their coherence and definite polarization state. Also they display much greater divergence and diffraction, while direct measurements of their amplitude and phase are relatively easy.

We then give a QO example to shape the horn aperture into a lens. Consider the geometry of Figure 1.11, which represents an axis-symmetric homogeneous solid dielectric horn with shaped aperture. Starting from the spherical wave front inside the dielectric horn, we define associated rays originating at point Q and refracting at surface $r(\theta)$ according to Snell's laws.

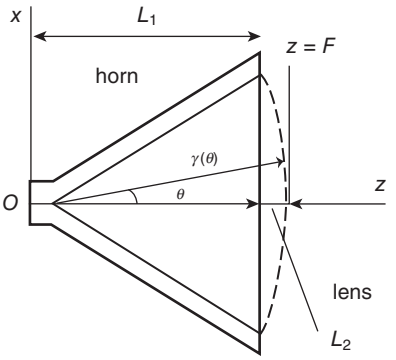

Figure 1.11. Geometry of axis-symmetric solid dielectric horn with shaped aperture for phase correction.

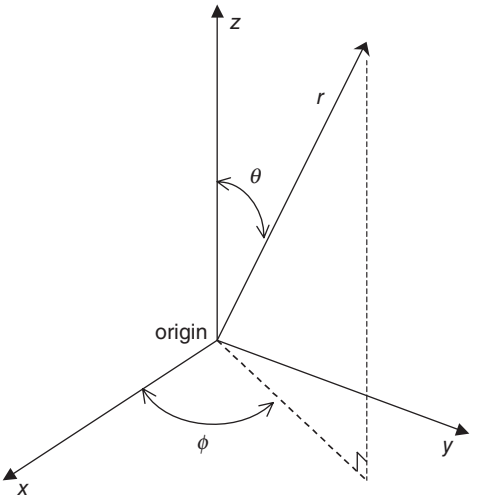

Figure 1.12. Spherical coordinate system.

The optical path along the rays from the origin O to plane $z = F = L_1 + L_2$ must be constant for all elevation angles θ and azimuth angles φ (Figs. 1.11 and 1.12)

$$r(\theta)\beta + F - r(\theta)\cos\theta = F\beta \tag{1.1}$$

Where r is the radius of the horn which is subject to the value of θ, and β is the normalized longitudinal propagation constant.

Equation (1.1) is written as if β were constant with z. Actually β changes with z but only from lens shape, in a region where the horn cross section dimensions are expected to be much larger than λ where β is almost constant and approaches $\varepsilon^{0.5}$. Under this assumption, rearranging (Eq. 1.1) we obtain

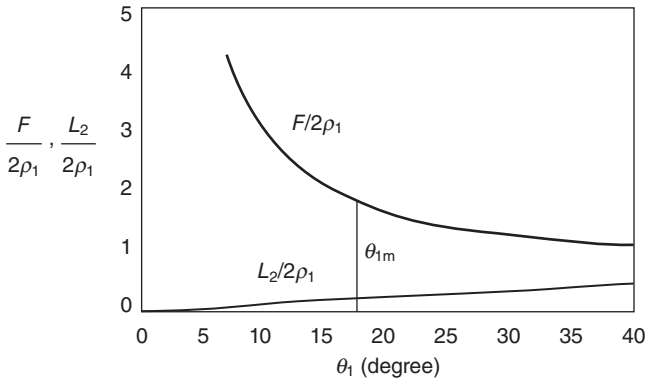

Figure 1.13. Lens depth and lens-horn depth to aperture ratio versus horn semi-fare angle θ for polystyrene material with dielectric constant ε = 2.5.

$$\boldsymbol{r}(\theta) = \frac{\boldsymbol{F}(\sqrt{\varepsilon} - 1)}{\sqrt{\varepsilon} - \cos\theta} \tag{1.2}$$

It's helpful to then express F in terms of the horn semi-flare angle θ_1 and the aperture radius ρ:

$$\boldsymbol{F} = \frac{\rho}{\sin\theta_1}\left[\frac{\sqrt{\varepsilon} - \cos\theta_1}{\sqrt{\varepsilon} - 1}\right] \tag{1.3}$$

Figure 1.13 shows the lens depth and lens-horn depth to aperture diameter ratio $L_2/2\rho_1$ and $F/2\rho_1$ versus horn semiflare angle θ_1. For the same flare angle $L_2/2\rho_1$ and $F/2\rho_1$ are larger for smaller values of ε. The ratio $L_2/2\rho_1$ grows faster with θ. The ratio $F/2\rho_1$ becomes more favorable as θ_1 increases, but there is an upper limit for this angle for two reasons:

Firstly, θ_1 must not exceed the value that allows the propagation of higher-order modes in the dielectric horn.

Secondly, the lens depth should not exceed the ellipse major semiaxis, that is

$$\theta_{1m} \leq \boldsymbol{arc}\cos\left[\frac{1}{\sqrt{\varepsilon}}\right] \tag{1.4}$$

For polystyrene material (ε = 2.5) we obtain θ = 51 degrees, far beyond the single mode operation condition.

The analysis and design of QO components could either lose accuracy in the range of the characteristic QO relationship between the wavelength and the size of the scatterer, or lead to high numerical complexity of the algorithms and hence prohibitively large computation times. Therefore, one would look in vain for the frequency

dependence of the gain of a reflector or lens antenna of realistic size computed with the method of moments or Finite-difference time-domain method (FDTD).

Exciting opportunities for the design of revolutionary new QO components and instruments are offered by emergent technological innovations, such as electromagnetic bandgap materials and meta-materials (also known as twice-negative and left-handed materials). For example, a QO prism made of bandgap material may display frequency and angular dependence of the incident beam deflection one hundred times stronger than that of a similar homogeneous prism [35]. Exotic designs of new QO lens antennas and beam waveguides made of meta-materials can be based on interesting effects including negative refraction [36]. Therefore the future of quasi optics is perfectly secure as long as electromagnetic waves are still used by the information society.

1.5 LENS ANTENNA DESIGN

The usual starting point for lens antenna design is to apply geometric optics. Here, a ray tracing approach is used, where the radiation is modeled as rays which radiate from an common origin, or source. Incidentally, this origin would be quite analogous to the antenna phase center. Of course, the validity of this simple approach is questionable because the lens typically lies within the near field region of the source or primary feed. GO is nevertheless though usually thought a valid starting point, particularly for predicting the properties of the main lobe wherein most of the radiation is contained. A quite surprisingly good agreement will be observed with measurement results in this main lobe regime. The sidelobes region, contrastingly, is not likely to be described with much accuracy.

Next, it is also simplest to design for lens cross sections which are circular (though they need not be). It then follows that the primary feed radiation pattern is circularly symmetric, though, again, it need not be. These starting assumptions removed dependence upon angle ϕ, the angle of rotation about the antenna axis of symmetry or boresight.

In principle though, the lens surface may be designed to accommodate asymmetries in the primary feed pattern, or ϕ angle dependency. These might be corrections for amplitude and also phase. In a more extreme case, a highly elliptical primary pattern (very different beamwidths in orthogonal planes, such as *E*-plane and *H*-plane) would require a lens cross section with similar ellipticity, although this seems a rare design objective and we present no examples. On the other hand, an antenna with a highly symmetric feed pattern but asymmetric secondary pattern is described in Chapter 5. This has a circular cross section, but still a ϕ dependency of the lens profile.

Returning to GO, its first principle is that the rays trace the flow of power between points. It follows from this that the aggregate flow of power through a closed surface comprises a bundle of such rays. Through such a bundle, or tube, power flow is constant across any cross section. The second pillar of GO is Fermat's principle which states that a ray's path is that which is of shortest length (or time) between any two given points. This underpins the optics of mirrors, reflection and refraction, and from which Snell's law may be derived.

A generalized design procedure for lenses can be listed as the following steps.

(i) Clarify the design objective for beamwidth and gain—this sets the required electrical dimensions.
(ii) Choose the operation frequency and bandwidth—the former sets physical dimensions.
(iii) Choose a suitable material (see Section 1.1.3)
(iv) Estimate the loss in the material. From this, dimensions may need to adjusted to realize the required gain.
(v) Determine the primary feed type, or other method of illumination.
(vi) Iterations as often as needed for fine-tuning the antenna performance.

For a lens which is properly designed, and acts as a collimating aperture, the directivity is determined by the aperture area. The gain will be lower than directivity by the sum of the various loss terms, including conductor loss, dielectric loss, and feed spillover loss (that proportion of the feed's radiated power which is not incident upon the lens surface). On aperture area, a simple rule of thumb is that doubling the aperture diameter will increase the gain by 6 dB, since the area of the aperture quadruples. For instance, an 12 cm lens fed by a 6 cm horn would add 6 dB to the gain of the horn, and a 24 cm lens would add 12 dB. Modest gain improvements take modest sizes, but beyond this big gain increases lead to physically large antennas and so for lenses working at the lower microwave frequencies the mass could become prohibitive. Of course, a 6 dB increase in gain will double the range of a communications system over a line-of-sight path.

Feed horn dimensions may be designed for the intended application, but in some cases it may be more practicable to use a commercial item.

If we start with a given primary feed, the beamwidth of the horn (usually smaller than the physical flare angle of the horn) will strongly influence the focal length of the lens. Looked at from the other point of view, if the focal length of the lens is the starting point, this determines the necessary feed properties. Clearly, longer focal lengths place the feed at a greater distance and so need a narrower beamwidth horn.

Approximations for the 3 dB beamwidths (respectively $\theta_{3dB}E$ and $\theta_{3dB}H$ for the *E*-plane and *H*-plane) often encountered in antenna theory are:

$$\theta_{3dB}E \approx \frac{57}{L_{E\lambda}} \text{ degrees}$$

$$\theta_{3dB}H \approx \frac{68}{L_{H\lambda}} \text{ degrees}$$

where $L_{E\lambda}$ is the aperture dimension in wavelengths along the *E*-plane direction, and $L_{H\lambda}$ is the aperture dimension in wavelengths along the *H*-plane direction. These relations reflect the well known inverse law between beamwidth dimension. Often, different numbers are used in the numerator on the right hand side, depending on assumptions

about the illumination edge taper. A stronger taper, or roll-off at the aperture limit, produces a wider beam. The above figures are typical for a pyramid type horn, and the wider *H*-plane beamwidth reflects the tendency for field distribution of the waveguide TE_{10} mode to decay along this direction.

Considering the shape of the lens, this depends on the refractive index n (the ratio of the phase velocity of propagation of a radio wave in a vacuum to that in the lens). A slow-wave lens antenna, as in optics, is one for which $n > 1$. A fast-wave lens antenna is one for which $n < 1$ but this does not have an optical analogy, at least for classical materials. Considering the Luneburg lens once again as an example, each point on its surface is the focal point for parallel radiation incident on the opposite side. Ideally, the dielectric constant ε_r of the material composing the lens falls from 2 at its center to 1 at its surface (or equivalently, the refractive index n falls from $\sqrt{2}$ to 1, according to

$$\boldsymbol{n} = \sqrt{\varepsilon_r} = \sqrt{2 - \left(\frac{\boldsymbol{r}}{\boldsymbol{R}}\right)^2}$$

where R is the radius of the lens. It should be added here that because the refractive index at the surface is (in theory at least) the same as that of the surrounding medium, no reflection occurs at the surface. In practice of course there must be a transition at a boundary between a real material with $n > 1$ and air with $n = 1$, but the closer to unity that the outer index can be made, the lower the reflection loss. In any case, the effect is sometimes over-estimated in spherical microwave lenses and the topic is taken up again in Chapter 6.

Returning to lens design in general we next calculate the lens curvature. In one approach the equation for lens curvature can be derived where there is just one refracting surface. The other surface is planar, and since rays enter it at normal incidence is does not produce refraction (Fig. 1.14). As noted above, we are now assuming rotational symmetry: there is no ϕ dependence and the problem reduces to two dimensions. The surface is most easily understood by equating all possible path lengths, including that along the central axis. In Figure 1.14, an arbitrary path has length r in air and l in the dielectric, while the axial path's components are the focal distance F in air and the maximum lens thickness T in the dielectric. Equating the electrical lengths yields:

$$nl + r = nT + F$$

This is also expressed in polar co-ordinates(r,θ) as

$$r = \frac{(n-1)F}{n\cos\theta - 1} \tag{1.5}$$

This equation defines a hyperbolic curve with eccentricity of n and where the origin coincides with the focus. Later, the profiles of other types of lenses will be described, for example, with two refractive surfaces. The design procedures follow a similar approach as for this simple case.

For collimation the optimum curvature is elliptical, but because we also know that a spherical curvature is commonly encountered in optics, we can say that a circle should

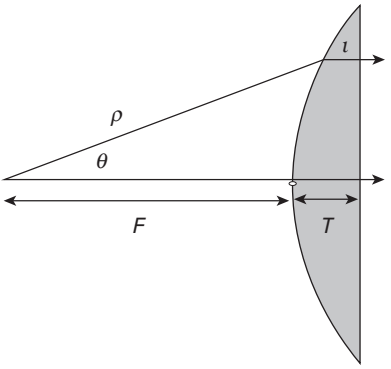

Figure 1.14. One-surface-refracting lens.

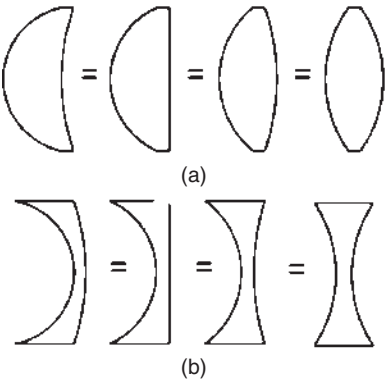

Figure 1.15. (a) equivalent optical lenses (b) equivalent metal lens antennas. All have the same focal length.

be a usable approximation to the planar-concave geometry of Figure 1.14. We can show that the circle is indeed a good fit if the focal length is more than twice the lens diameter, that is, it is an *f*/2 lens. From this geometry it can be shown that the beamwidth of the feed shouldn't exceed 28 degrees, requiring its aperture dimension to be 2 wavelengths or greater.

The radius of curvature R of the two lens surfaces is calculated from an optical formula:

$$\frac{1}{\boldsymbol{f}} = (\boldsymbol{n}-1)\left(\frac{1}{\boldsymbol{R}_1} - \frac{1}{\boldsymbol{R}_2}\right)$$

where a negative radius denotes a concave surface. All combinations of R_1 and R_2 which satisfy the formula are equivalent, as shown in Figure 1.15.

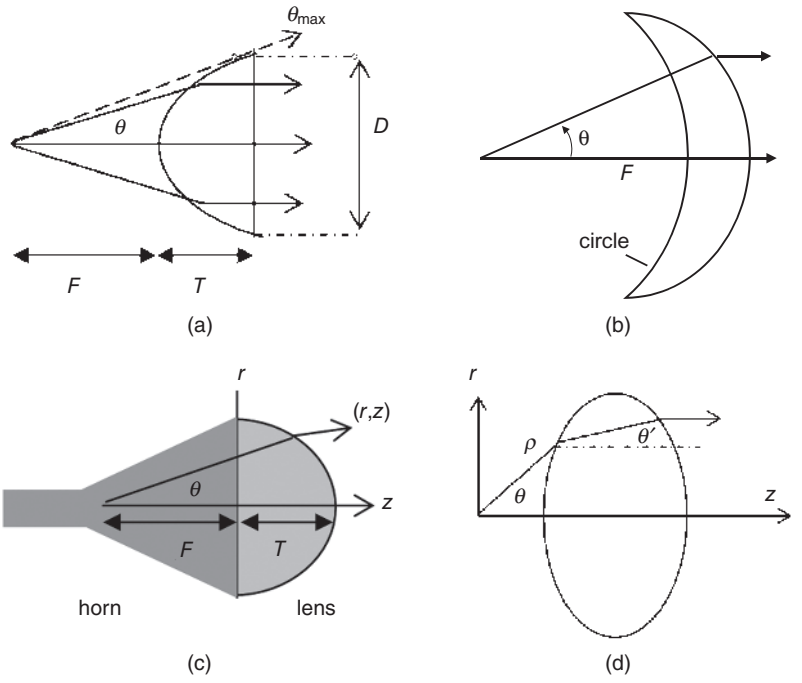

Figure 1.16. Types of lens: (a) type *a*; (b) type *b*; (c) type *c*; (d) type *d*.

The over-arching objective of the collimating lens, like that of the parabolic reflector, is an aperture exhibiting a constant phase front. To this end, the four most common lens types will be reviewed, as shown in Figure 1.16. Types *a* and *b* have one refracting surface, and one where rays pass at normal incidence. We have already encountered type *a* above and in Figure 1.14. In contrast, in type *b*, it is the surface on the opposite side from the feed at which refraction takes place, and the facing side is spherical. Types *c* and *d* lenses are often called "dual-surface lenses" because both are used to produce a required amount of refraction which together produce collimation and the required constant phase front. Type *d* has two similar refracting surfaces while Type *c* has two dissimilar surfaces (one is plane), but can be identified as a sub-class of type *d* and as one which is favorable for placing directly in the aperture of a horn, as illustrated.

Two formulations are now useful for describing each type of lens. These are a formula for the lens thickness, and another for the surface, although they are really equivalents. The profile for the type *a* lens has already been covered above. Its thickness *T*, relative to its diameter *D*, is given by:

$$\frac{T}{D} = \sqrt{\left\{\frac{1}{n^2}\left(\frac{F}{D}\right)^2 + \frac{1}{4n(n+1)}\right\}} - \frac{F}{nD}$$

Moving on to the type *b* lens, the surface facing the feed is spherical, while the opposite face has a profile described by the polar equation:

$$r = \frac{(n-1)}{\cos\theta + n} F$$

and thickness:

$$\frac{T}{D} = \frac{1}{2\sqrt{(n^2-1)}}$$

If the type a lens is intended to be placed in the aperture of a horn, and in contact with it, the angle θ_{max}—Fig. 1.16a—must exceed the horn's interior angle of taper, where

$$\theta_{max} = \cos^{-1}\left(\frac{1}{n}\right)$$

If this condition isn't met, a physical contact can't be made across the full aperture of the horn. This need not necessarily be a problem, but would require an additional support structure between the horn and lens, a longer structure, and could give rise to excessive spill-over radiation unless the horn's (primary feed) pattern is carefully chosen.

For the type *c* lens, as a matter of convenience, we use a radius *r* along the transverse axis which is orthogonal to the usual lens axis *z*. The shaped lens profile is then given by *r* and *z*, both expressed as functions of angle θ:

$$r = \frac{(n-1)T + (n^2-1)F\sec\theta - FS\tan\theta}{\left(\frac{n^2}{\sin\theta} - S\right)} \tag{1.6}$$

and

$$z = (r - F\tan\theta)S \tag{1.7}$$

where

$$S = \sqrt{\left\{\left(\frac{n}{\sin\theta}\right)^2 - 1\right\}}$$

The axial thickness of the type *c* lens, again relative to diameter *D*, is

$$\frac{T}{D} = \left[\sqrt{\left\{1 + \frac{1}{\left(\frac{2F}{D}\right)^2}\right\}} - 1\right] \frac{\frac{F}{D}}{n-1} \tag{1.8}$$

The equations defining the surfaces of type *d* lenses cannot be expressed as directly as with the preceding 3 cases. Instead, they are related through simultaneous differential equations. These have been expressed by Olver et al. [18] as:

$$\frac{d\rho}{d\theta} = \frac{n\rho\sin(\theta-\theta')}{n\cos(\theta-\theta')-1}$$

$$\frac{dr}{d\theta'} = \frac{P(\theta')\sin\theta' r_{\max}^2}{2r\int_0^{\theta'_{\max}} \rho(\theta')\sin\theta' d\theta'}$$

$$\frac{dz}{dr} = -\tan\left\{\theta' + \tan^{-1}\left(\frac{\sin\theta'}{n\cos\theta'}\right)\right\}$$

where $P(\theta')$ is the radiated power per unit solid angle, and in the direction:

$$\theta' = \theta - \frac{\pi}{2} + \tan^{-1}\left(\rho\frac{d\theta}{d\rho}\right) + \sin^{-1}\frac{1}{n\sqrt{\left\{1+\left(\rho\frac{d\theta}{d\rho}\right)^2\right\}}}$$

The axial thickness T of a type *d* lens is given [18] by:

$$\frac{T}{D} = \sqrt{\left\{\frac{1}{n^2}\left(\frac{F}{D}\right)^2 + \frac{1}{4n(n-1)}\right\}} - \frac{F}{nD}$$

Unsurprisingly, the type *d* lens, as well as being of more complex design, entails more fabrication stages compared to its type *c* counterpart, and possibly offers little, if any, performance advantage.

The relative permittivity of the lens material shouldn't be less than a certain minimum value if the primary feed is intended to be a horn type in contact with the lens. In this context, a long horn with a narrow flare angle would be needed with very low constant lenses which of necessity are physically thick (these fall into the low density foam category with $\varepsilon_r < 1.5$). Such a horn-lens combination may offer minimal advantage compared to the horn on its own, and a better combination would use a higher relative permittivity, for example, >1.7. More details can be found in Reference 37.

One of the main disadvantages of dielectric lenses is their bulk at lower microwave frequencies. To overcome this, the thickness of a solid-dielectric lens can be reduced by removing slabs of integral-wavelength thickness at periodic intervals called *zones*. Applying this to a type *c* lens gives rise to the profile shown in Figure 1.17. Here, a point at transverse radius r and axial distance z is shown.

When the zoning principle is applied across the lens surface the optical-path length differs by one wavelength between adjacent zones. Starting from the center and increasing radial distance r, the next zone interval is the point at which the lens thickness has reduced by one wavelength. Hence the next zone commences with an increase in

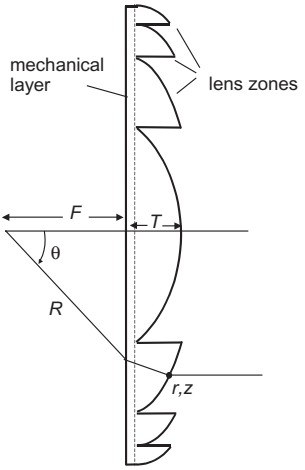

Figure 1.17. Zoned lens.

thickness of the same amount, which is $\lambda_0/(n\text{-}1)$. The minimum physical lens thickness needs to be at least a little larger than this value to provide a mechanical support layer, as indicated on the left side in Figure 1.17. For N zones, the path through the outer zone is $\lambda_0(N\text{-}1)$. The zoned lens is hence a limited bandwidth device, and becomes more so as its diameter increases and more zones are used. Hence this approach detracts from what is otherwise an inherently wideband device.

From Figure 1.17, the equations for the profile in terms of both angle θ and R are just modified versions of those encountered for the continuous surface type c lens, and are:

$$r = R\sin\theta + \frac{z}{S}$$

and

$$z = \frac{(N-1)\lambda + (n-1)T + F - R}{\frac{1}{S}\left(\frac{n}{\sin\theta}\right)^2 - 1}$$

where $N = 1,2,3. \ldots$ etc counting from the lens center, and S is the same as that in (Eq. 1.8).

Zoned lenses are best used at lower microwave frequencies rather than at millimeter wave frequencies. In the former case the mass saving can be significant and it is worth the extra fabrication complexity, so long as bandwidth requirements are not great. A subtle disadvantage of zoning is that aperture blockage is introduced by the discontinuities between zones, an effect which is a strong function of *f/D* value [38].

Another development of the zoned lens is the phase correcting Fresnel zone plate lens (Fig. 1.18). Here the manufacturing process is simplified because the curvature of

Figure 1.18. Phase Correcting Fresnel Zone Plate Lens.

a conventional lens (zoned or otherwise) is dispensed with and a set of radial grooves at discrete depths used instead. The radii of the grooves are given by:

$$r_i = \sqrt{2Fi\frac{\lambda_0}{p} + i\left(\frac{\lambda_0}{p}\right)^2} \quad i = 1, 2 \ldots$$

and the thickness of the step s by:

$$s = \frac{\lambda_0}{p\left(\sqrt{\varepsilon_r} - 1\right)}$$

where F is focal length, λ_0 the free space wavelength and p is an integer which defines the number of steps and hence the granularity of the surface. For example, for $p = 2$ there are 2 corrections per wavelength or a 180° phase correction, for $p = 4$ there are 4 corrections per wavelength or a 90° phase correction and so on. (For p = infinity the steps are blended out into a continuous curved surface.)

Metal plate lenses, encountered above in Figure 1.2, have been used as a potentially less massive alternative to either smooth or zoned dielectric lenses, with a different set of strengths and weaknesses in degrees of freedom for the design—among these being bandwidth and polarization.

1.6 METAMATERIAL LENS

Metamaterials are artificial composite structures with artificial elements (much smaller than the wavelength of electromagnetic propagation) situated within a carrier medium. The subject attracted significant interest since practical implementation solutions have emerged. Also, research work shows that antenna gain can be enhanced by using metamaterials as antenna substrates [39].

These materials can be designed with arbitrary permeability and permittivity [40]. Left-handed materials are characterized by a negative permittivity and a negative permeability- at least across a portion of the electromagnetic frequency spectrum. As a consequence, the refractive index of a metamaterial can also be negative across that portion of the spectrum. In practical terms, materials with a negative index of refraction are capable of refracting propagating electromagnetic waves incident upon the metamaterial in a direction opposite to that of the case where the wave was incident upon a material having a positive index of refraction (the inverse of Snell's law of refraction

in optics). If the wavelength of the electromagnetic energy is relatively large compared to the individual structural elements of the metamaterial, then the electromagnetic energy will respond as if the metamaterial is actually a homogeneous material.

As these materials can exhibit phase and group velocities of opposite signs and a negative refractive index in certain frequency ranges, both of these characteristics offer a new design concept for lens antenna feeding.

One of the approaches starts from the equivalent transmission line model and artificially loads a host line with a dual periodic structure consisting of series capacitors and shunt inductors [41]. The length of the period and the values of the capacitors and inductors determine the frequency band in which the material has this double negative behavior.

An example of such structures is in arrays of wires and split-ring resonators [42, 43]. These three-dimensional structures are complicated and are difficult to apply to RF and microwave circuits. A more practical implementation uses transmission lines periodically loaded with lumped element networks [44, 45].

The starting point is the transmission line model presented in Figure 1.19a. The equivalence between the distributed L and C for the transmission line and the permittivity and permeability of the medium is expressed as $\varepsilon = C$, $\mu = L$. By periodically loading this transmission line with its dual in Figure 1.19b, the values of ε and μ change as follows [44]:

$$\varepsilon_{eff} = \varepsilon - \frac{1}{\omega^2 Ld} \quad \mu_{eff} = \mu - \frac{1}{\omega^2 Cd} \tag{1.9}$$

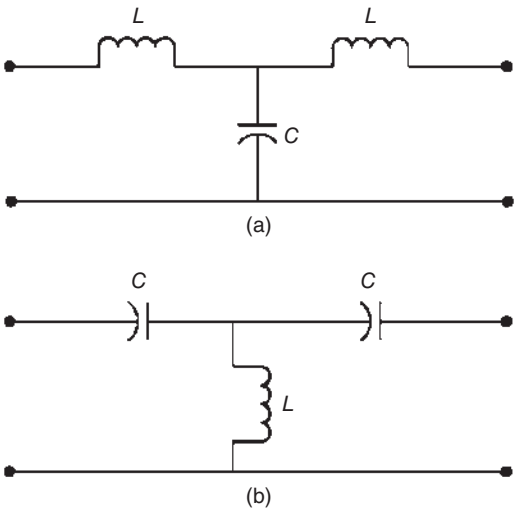

Figure 1.19. (a) *L*-*C*-*L* and (b) *C*-*L*-*C* transmission line models.

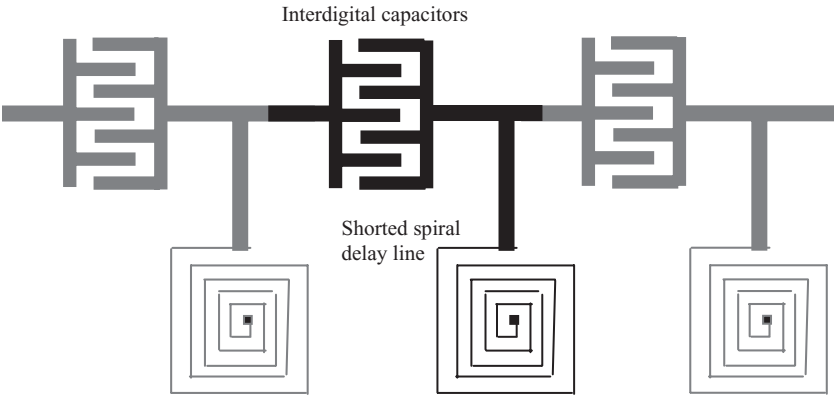

Figure 1.20. Periodic structure of three unit cells.

where ε and μ are the distributed inductance and capacitance of the host transmission line respectively. It is clear from Equation (1.9) that for certain values of *L, C* and *d*, the effective permittivity and permeability of the medium becomes negative for some frequency ranges. In these ranges, the refractive index is negative and the phase and group velocities have opposite signs.

In Figure 1.20, three unit-cell circuit structures are repeated periodically along the microstrip line. A unit-cell circuit, in the structure, consists of one or more electrical components that are repeated—in this case disposed along the microstrip transmission line. In the structure in Figure 1.20 above, series interdigital capacitors are placed periodically along the line and T-junctions between each of the capacitors connect the microstrip line to shorted spiral stub delay lines that are, in turn, connected to ground by vias. The microstrip structure of one capacitor, one spiral inductor and the associated ground via, form the unit-cell circuit structure of Figure 1.20.

Structures such as Figure 1.20 can be used in leaky-wave antennas (as opposed to phased array antennas), which have been designed to operate at frequencies of up to approximately 6.0 GHz [46]. With certain modifications, these metamaterials can be used at relatively high frequencies, such as those frequencies useful in millimeter wave communications applications [47]. For instance, the unit-cell circuit structure of Figure 1.20 can be reduced to a size much smaller than the effective wavelength of the signal. To achieve a high-performance transmission line impedance at a particular frequency, the physical size and positioning of unit cells in the metamaterial microstrip line needs to be carefully considered.

High-gain printed arrays have previously relied on a signal-feed/delay line architecture that resulted in a biconvex, or *Fresnel lens* for focusing the microwaves [47]. The use of such lens architectures has resulted in microwave radiation patterns having relatively poor sidelobe performance due to attenuation as the wave passed through the lens. Specifically, the signal passing through the central portion of the lens tended to be attenuated to a greater degree than the signal passing through the edges of the lens.

This resulted in an aperture distribution function that was "darker" in the center of the aperture and "brighter" near the edges. The diffraction pattern of this function results in significant sidelobes (the diffraction or far-field radiation pattern is the two-dimensional Fourier transform of the aperture distribution function). While placing signal delay lines in the lens portion of the system could reduce the sidelobes and, as a result, increase the performance of a phased-array system, this was deemed to be limited in its usefulness because, by including such delay lines, the operating bandwidth of the phased-array system was reduced.

However, instead of a biconvex lens, a metamaterial can be used to create a biconcave lens (by means of controlling the effective refractive index of the material) for focusing the wave transmitted by the antenna. As a result, a wave passing through the center of the lens is attenuated to a lesser degree relative to the edges of the lens (the aperture is now brighter at the center and darker near the edges), thus significantly reducing the amplitude of the sidelobes of the antenna while, at the same time, retaining a relatively wide useful bandwidth.

The metamaterial lens is used as an efficient coupler to the external radiation, focusing radiation along or from a microstrip transmission line into transmitting and receiving components. Hence, it can be designed as an input device. In addition, it can enhance the amplitude of evanescent waves, as well as correct the phase of propagating waves.

A meta-material lens is made using composite right/left handed transmission line (CRLH-TL) [48]. The potential of the shaped metamaterial lens has been investigated for wide angle beam scanning [49]. One example is a meta-material lens antenna using dielectric resonators for wide angle beam scanning. The lens antenna is composed of the radiator, the parallel plate waveguide and the meta-material lens.

Figure 1.21 shows an unit cell of the meta-material lens. The unit cell is composed of the parallel plate waveguide with $\varepsilon_r = 2.2$ and the dielectric resonator with $\varepsilon_r = 38$, thickness is $h = 2.03$ mm and the diameter is $a = 5.1$ mm. The distance of the parallel

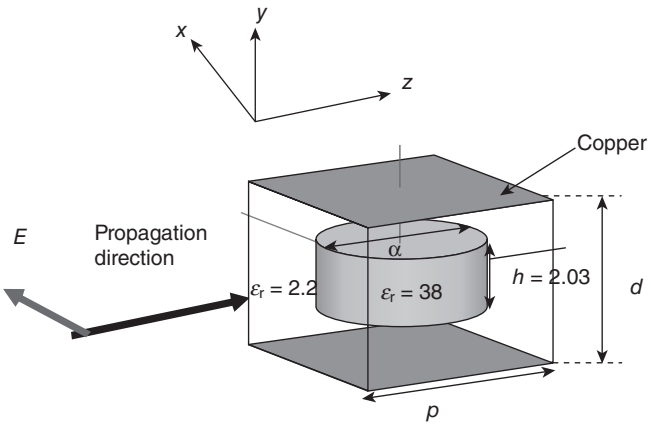

Figure 1.21. Configuration of unit cell of the metamaterial lens (©2010 IEEE [49]).

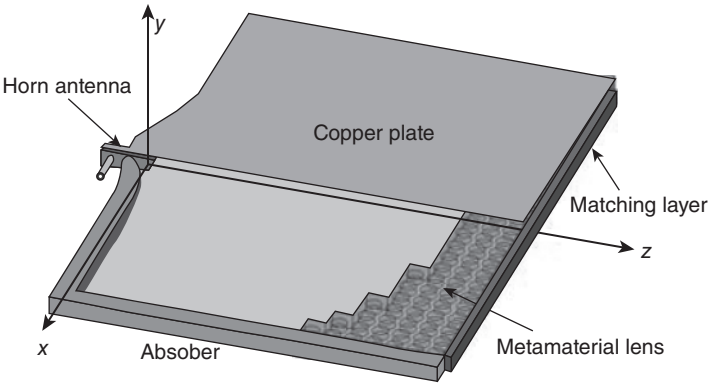

Figure 1.22. Configuration of the metamaterial lens antenna for wide angle beam scanning (©2010 IEEE [49]).

plate is d. The excitation mode of the parallel plate waveguide is TE_1 mode in order to excite $TE_{01\delta}$ mode of the disk type dielectric resonator. The effective permittivity ε_{eff} and permeability μ_{eff} are shown in Figure 1.22.

The frequency at $\varepsilon_{eff} = 0$ increases as d decreases because the cut-off frequency shifts to a higher frequency. When $d = 5.1$ mm, negative values of ε_{eff} and μ_{eff} are obtained below 11.5 GHz and the refractive index n becomes negative value. Here, $n = -1$ is obtained around at 11 GHz. Figure 1.22 shows the configuration of the meta-material lens antenna composed of the radiator, the parallel plate waveguide and the metamaterial lens. The number of unit cells is 100, $f/D = 0.5$ and the lens aperture is 156 mm (about 5.7 λ). The minimum thickness of the metamaterial lens along z axis is three cells. The matching layer is set on the aperture of the lens for the impedance matching between the metamaterial lens and the air. The absorber materials are set around the lens antenna for reduction of the multiple reflections in the parallel plate waveguide. The parallel plate waveguide between the radiator and the metamaterial lens is filled by dielectric material with $\varepsilon_r = 10.2$.

1.7 PLANAR LENS OR PHASE-SHIFTING SURFACE

A concept gaining ground since the mid 1990s has been the planar lens [50] or phase-shifting collimating surface. Like the reflect-array, the planar lens comprises a surface of discrete radiating elements configured to yield a phase distribution which exhibits a collimating effect. While the origin of the "reflect-array" moniker would be self-evident, the equivalent "lens-array" appears not to have come widely into use. Notwithstanding this nomenclature, the two techniques are closely related, just as the reflector and lens antennas are related: each exhibits a first focus at which a primary feed is placed, and a second focus at an infinite distance.

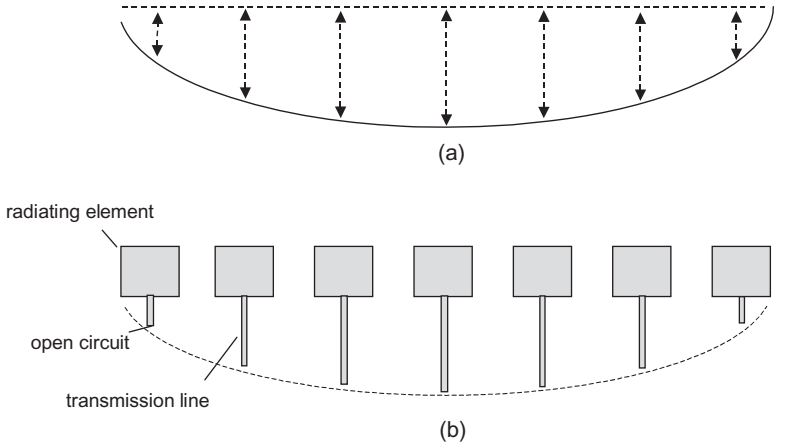

Figure 1.23. Reflect-array concept: (a) path lengths across aperture of parabolic reflector, and (b) discretized equivalent using radiating elements and transmission lines.

1.7.1 Reflect Array

The reflect-array has received rather more attention than its lens-like equivalent and so it's worth proceeding with a very short review of this technology. The principle of operation of the planar lens should then be more easily grasped.

The essential property of the reflect array is to re-radiate the incident field of a source, or primary feed, in a manner which yields a constant-phase aperture and thus a collimated beam. While collimation is achieved by a parabolic reflector owing to its curvature, the reflect array utilizes a discrete set of array elements, distributed across a planar aperture, whose phase responses are suitably tailored. The two cases are compared in Figure 1.23a,b. While a linear array is shown the same phase shifting principle could apply also across two dimensions. The radiating elements could be any convenient antenna (in some early reflect arrays waveguide horns were used) although a popular and practical type would be a printed dipole, patch or similar. A means of varying the phase response of each radiator (i.e., the phase of the reflected field compared to the incident field), and one which is perhaps easiest to visualize, is the series addition of a short or open-circuited transmission line. Then, varying the length of this line varies the phase of the element's re-radiated field.

Considering printed radiating elements it is easy to see how these can conveniently be integrated with printed microstrip transmission lines whose lengths are chosen to produce the required aperture phase distribution, albeit in a discretized manner. Now, open circuited microstrip lines exhibit some disadvantages: consumption of circuit real estate, a tendency to produce unhelpful radiation at the open circuit stub, and circuit loss. These drawbacks can to some extent be ameliorated by use of aperture coupled patches so that parasitic radiation can be suppressed on the opposite surface to the radiating aperture. Alternatively, the microstrip lines can be dispensed with altogether

if alteration of some other dimension (e.g., patch length and width) can be contrived to generate an adequate variation in phase.

A cited advantage of reflect arrays includes that of fabricating a reflecting, collimating surface without recourse to the perceived manufacturing cost of fabricating a parabolic dish. Now, while dishes up to a certain size (say 0.5 to 1.0 m, as used for satellite TV) are nowadays remarkably low in cost, other properties of reflect arrays compared to parabolic reflectors should also be set out. The reflect array allows for further manipulation of the aperture distribution, for example by integrating active phase shifters or amplifiers to the array circuit. Radiating elements may be tuned to particular frequencies or to introduce polarizing effects (e.g., yield circular polarization from a linear polarized feed). In Reference 51 a switched beam variant was reported, whereby the phase distribution across the aperture was altered by mechanical adjustment of one of the laminates.

Furthermore, beam shaping can be achieved by imposition of an arbitrary phase and amplitude distribution across the array, and this can be achieved at low cost and for low production volumes should the array be fabricated using printed circuit technology. The reflect array has also established interest as a stowable or foldable antenna; this has been of particular interest in space communications where large apertures might be stowed in relatively small volumes for launch, then unfurled for deployment in orbit. Some remarkable examples of experimental antennas for space have been inflatable reflect arrays developed at Jet Propulsion Laboratory [52, 53]. Reflect arrays of course are not without disadvantages. Perhaps the most prominent among these are the inherent low bandwidth which is caused by the frequency dependence of delay-lines (if used) or other phase altering property of the elemental radiators.

Other types of reflect array may be illuminated from a distance and so both foci lie at infinity. These may also phase modulated so as to impart a unique code on the reflected signal [54] although these reflectors act as transponders rather than antennas in the present context. One such device is shown in Figure 1.24 where the radiating

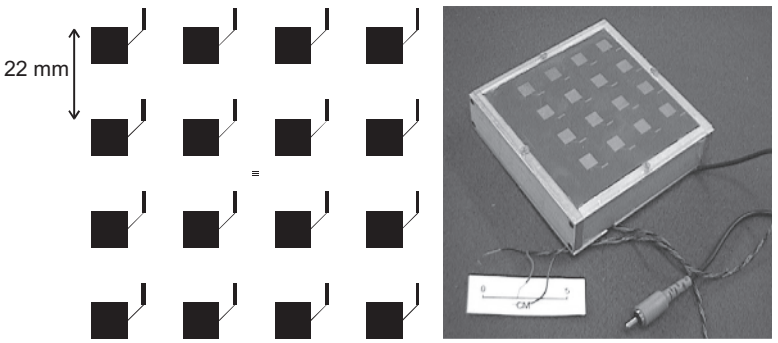

Figure 1.24. An active reflect-array (a) circuit for x-band, (b) assembled transponder.

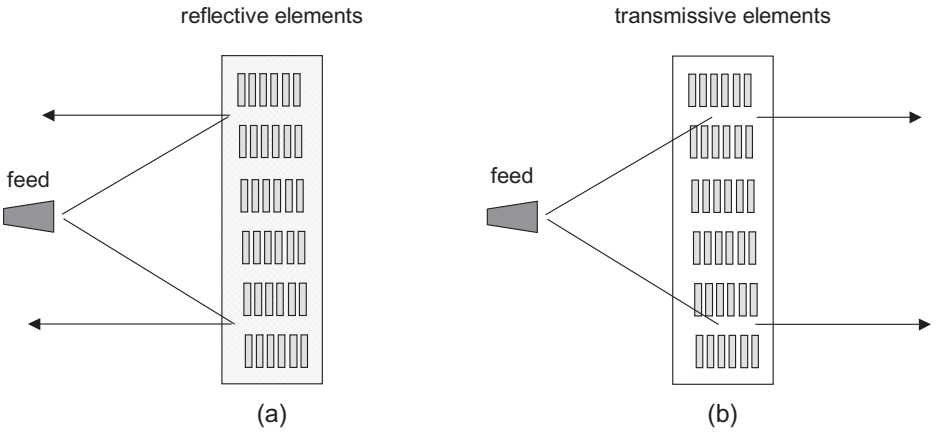

Figure 1.25. Reflect array (a) compared to lens array (b).

elements are visible and the active elements are housed on a second laminate which is aperture-coupled to the radiating layer.

1.7.2 Planar Lens or Lens Array

Having introduced the basic properties of the quite well established and studied reflect array, the principle of the planar lens, or as has been coined here "lens array," should be apparent. The terms "discrete lens" and "transmit array" have also been used. Where the radiating elements of the reflect array are replaced with transmissive elements (Fig. 1.25), and so long as elemental phase distribution is retained, the surface resembles a lens rather than reflector. Put another way, the radiating elements are now required to forward scatter rather than back scatter. In practice, this would likely be achieved by dispensing with the ground plane associated with the reflect-array's patch antennas, and optimizing the forward scattering efficiency of the elements. This would lead to a single layer lens array. Suitable radiating elements could then closely resemble those commonly encountered in frequency selective surfaces, for example, loop, star, slot, ring, or dipole types [55]. A difference however is that the elements of the single layer lens array will not be of uniform dimension, since the phase of the forward scattered component must be a function of the path distance to the primary feed. Ideally, it should be possible to set the phase response of each element within the range 0° to 360° which is not always straightforward depending on the type of radiating element chosen. Another type of radiator reported is the stacked (multi-layer) patch, where several degrees of freedom are available to help tune to the desired phase response. In Reference 56 three metallic and two dielectric layers were used to realize phase shifting surfaces at 30 GHz.

Alternatively, a dual-layer lens array can be used where one array acts as a receiving layer and each element is connected to a counterpart in a second, transmitting array.

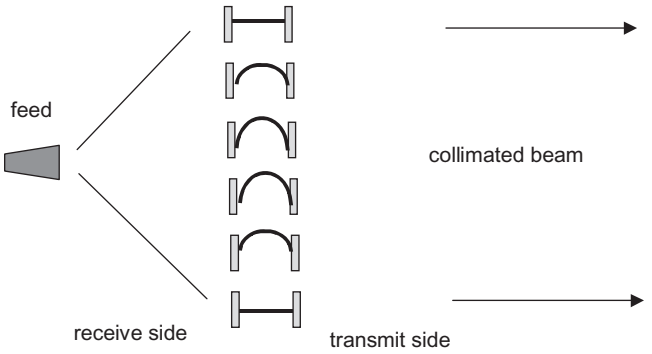

Figure 1.26. Two layer lens array with interconnecting lines which determine phase.

The lengths of the interconnecting lines determine the required phase relationship between transmitting and receiving elements according to their location in the array planes (Fig. 1.26). Here it is more straightforward to set the phase relationship between the two interconnected elements: the length of the transmission line is increased or decreased as necessary, although this does lead to the disadvantages of ohmic loss and the consumption of circuit real estate.

A subtle effect that needs to be considered in lens arrays is that both the element frequency response and the phase of its transfer function tend to vary with the incident angle of the incident wave (the incidence angle with respect to the feed), particularly for short *f/D* ratios. For *f/D* much greater than 1 the variation of incidence isn't very great and its effect might justifiably be ignored.

In Reference 57 a variant was reported whereby the intermediate layer between receive and transmit printed antennas comprised a co-planar-waveguide resonator. The properties of this resonator determined the phase relationship between the two antennas and so acted in lieu of the more simplistic transmission line interconnection illustrated above. Furthermore, the resonator exhibited filter properties and so the term "antenna-filter-antenna" was coined for this frequency selective radiating element. Phase ranges of only 0° to 180° were achieved for a given antenna element type, but the full 0° to 360° range was achieved by combining two different types across the planar lens aperture. Abbaspour-Tamijani et al. [57] reported an experimental 3-in.- diameter lens array with measured gain 25.6 dBi at 35.3 GHz and so with an effective insertion loss of 3.5 dB.

Another type of planar lens antenna is the *Fresnel zone-plane lens* (Fig. 1.27). The origin of this lens is from its optical equivalent where a flat lens was sought. Its principle of operation is that adjacent rings have a mean phase difference of $\pi/2$- these are Fresnel zones. By blocking out alternate zones, those remaining zones have in-phase average path lengths. Like the zoned dielectric lens, the zone-plate is bandwidth limited because its design is fixed for a particular frequency. Also, the zones can be chosen to yield two

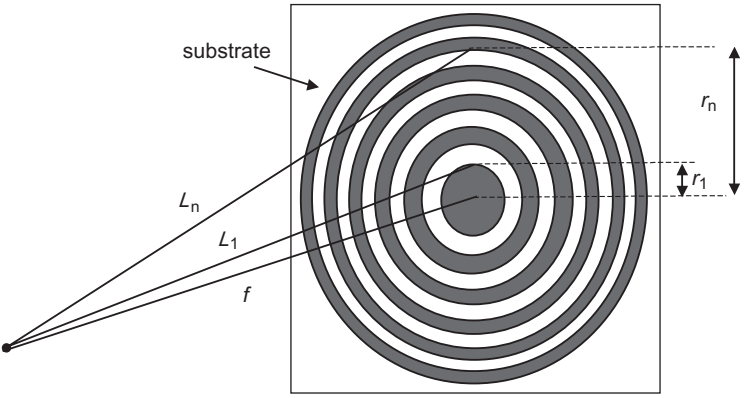

Figure 1.27. A Fresnel zone plate lens.

arbitrary foci, or where one focus is at infinity the zone plate is useful as a lens antenna. The lens radii can be derived from straightforward use of Pythagoras's theorem and Figure 1.27. Here, the path length L at each ring edge increments by one half wavelength, thus

$$L_n = f + n\frac{\lambda}{2}$$

where f is the focal distance and n is a counter = 1,2, . . .
and so:

$$r_n^2 = f^2 + \left(\frac{n\lambda}{2}\right)^2$$

Furthermore, for $f >> \lambda$, such as might occur in optics, we can approximate $rn \approx \sqrt{nf\lambda}$.

The chief advantages of the zone plate, as a lens antenna, is the convenience of its flat structure and the simplicity of manufacture. Such a plate can easily be fabricated as a printed circuit, for example. Of course, its profound disadvantage is that the blockage of alternate zones rejects half the available power from the system. However, the concept has been adapted for microwave frequencies by using dielectric rings of alternating height where the adjacent zones' thicknesses differ by one half wavelength, and the metal (blocking) rings are dispensed with. This recovers the otherwise missing half of the available energy, but the phase relationship between rings (zones) is still imperfect, there being a 90° discontinuity at each boundary. These phase errors are reduced by reducing the granularity of the steps and leads to the phase correcting Fresnel zone plate lens Figure 1.18 discussed above, which typically uses more steps and more closely resembles the zoned dielectric lens.

In all these versions the complete zone-plate lens is made out of a single dielectric material. A recent alternative construction, based on the same principle, uses two different dielectric materials. In this version all of the rings have exactly the same thickness, but the phase-shifted rings are composed of the second dielectric material. The advantage of this structure is that the surface is completely flat instead of possessing small ridges. A recent article by J. C. Wiltse [58] discusses the operation of the zone-plate lens for millimeter waves and describes the various versions mentioned above. Another comprehensive summary is found in Reference 59.

Unsurprisingly, there exists a close analogue in reflector antennas with the Fresnel zone reflector which employs a similar zoning of reflective rather than diffractive bands.

The concepts of the Fresnel zone plate lens (Fig. 1.26) and the phase shifting surface lens were cleverly combined in Reference 60 where a phase shifting surface was used instead of the otherwise opaque metal zones, and a significant fraction of the lens area was not metalized at all. This structure was called a phase-correcting phase shifting surface (PSS) lens antenna and Gagnon et al. [60] compared it with three other lens types: dielectric plano-hyperbolic lens antenna, 90° phase-correcting Fresnel zone plate antenna. (Fig. 1.18) and Fresnel zone plate antenna (Fig. 1.27), all with a diameter of 152 mm and *f/D* ratio 0.5. Measurements on the 4 types were carried out in the region 30 GHz. The PSS lens of Gagnon et al. [60] outperformed all but the plano-hyperbolic dielectric lens antenna, falling short by just 0.3 dB of gain. However, it exhibited a weight reduction by a factor of almost ten and a forty-fold thickness reduction. The chief disadvantage was limited bandwidth, being 7% at 1 dB.

1.8 APPLICATIONS

Lens antennas can find application in a wide range of environments; a few are listed below:

1. Fixed wireless services such as telephony and internet. These services might be combined.
2. Satellite television (receive only service) with the possibility of multiple beams and hence using multiple satellites, without the need for motorized feeds.
3. Ultra Small and Very Small Aperture Terminals (USAT/VSAT) for two-way satellite communications.
4. In radar, for active or passive signal scanning of a wide area, for security purposes or for automotive collision avoidance radar such as is used in bands around 77 GHz.
5. Radio Frequency Identification (RFID).
6. Multi-beam antennas. In wireless local area network (WLAN) applications, multiple point-to-point communication links can be arranged using the same antenna, thus eliminating the slow-down of data speed when many nodes are transmitting in an omni-directional fashion and thus interfering with each other.

7. In compact radio transceivers where the electronic components and modem are protected in a casing behind the antenna aperture, offering a measure of isolation from the environment. Such an enclosed antenna is also excellent in repeater systems, where received and transmitted signals tend not to disturb each other.

Also, voltage standing wave ratio (VSWR) measurements reveal that the lens antenna is equally well-suited as a transmitter as a receiver. The reflection coefficient at the primary feed should be very low and so is not particularly likely to reflect much transmitted power back toward the power amplifier.

The compactness of lens antennas and the ease with which multi-beam variants can be produced makes them very attractive for exploiting the large bandwidths available at millimeter wave frequencies and thus suitable for very high data rate and spectrally efficient communications. This theme will occur several times throughout the following chapters.

1.9 ANTENNA MEASUREMENTS

Aside from an antenna's physical properties (mass, dimensions and so on) its electrical properties are of most interest to engineers and the measurement of which merits careful consideration. Also setting aside the property of return loss, which would entail the use of a vector network analyzer in a calibrated, single port measurement, it is the measurement of antenna radiation patterns which are of most interest. Approaches to measurement of radiation patterns fall into several broad areas such as indoor, outdoor, near field and far field methods. A summary may be found in Chapter 17 of Reference 17.

Outdoor ranges are, almost by definition, not protected from the environment (precipitation, interference), while indoor ranges offer limited inter-antenna separation. Indoor ranges use an anechoic interior lining to provide a non-reflective measurement environment . Two basic forms of anechoic chambers are rectangular and tapered box types; the latter are used more for low radio frequencies, for example, below 1 GHz.

1.9.1 Radiation Pattern Measurement

The radiation pattern of an antenna is three-dimensional over a sphere surrounding the antenna. Because it is not always practical to measure a three-dimensional pattern, a number of two-dimensional patterns (referred to as pattern cuts) are often measured. Different types of antenna positioners can perform this, such as Elevation-over-Azimuth, Azimuth-over-Elevation, or Roll-over-Azimuth mounts. Antenna directivity can be derived from the measured radiation pattern. This entails the numerical integration of the radiation intensity over all of space and so requires an adequate sampling over a spherical surface, which has implications for the time required to measure what can be a large data set. Alternatively, directivity might be inferred from two orthogonal planes of data, where interpolation is used for the space between and some loss of accuracy must be expected. For highly directive antennas (many lens antennas will fall in this

category) measurement time may justifiably be reduced by capturing data over just the main lobe, again with some loss of accuracy.

1.9.2 Gain Measurement

Gain can be measured using two basic methods: either by comparison with a known calibration standard (e.g., a "standard horn"), or by calculation using the Friis transmission equation. The latter, also called the absolute gain method, requires that either the transmit and receive antennas are identical, or if they are different then three antennas and three measurements are needed to formulate a set of three simultaneous equations whose solution determines the gain of the antenna-under-test (AUT).

1.9.3 Polarization Measurement

A straightforward way to measure polarization entails two measurements using orthogonally polarized linear probes, which might be vertically and horizontally polarized (but need not be). In a second method, a single probe mechanically spins (perhaps quite quickly, e.g., a few Hz) which is quite useful for direct measurement of the axial ratio of a notionally circular polarized AUT.

1.9.4 Anechoic Chambers and Ranges

In choosing a measurement method one might best begin with an assessment of how conveniently a far field measurement could be performed. Here one would start with a calculation of the far field condition:

$$r_{far} > \frac{2D^2}{\lambda}$$

That is, the far field (*Fraunhofer*) zone of the antenna's radiation pattern can be approximately considered to begin at a distance not less than r_{far} above where D is the physical aperture diameter and λ is wavelength. More strictly, D is the diameter of a minimum radius sphere which wholly encloses the antenna structure. Furthermore, this approximation derives from the pragmatic observation that at this distance the maximum phase error between the observer and any part of the antenna aperture, of $\pi/8$ radians, would make little difference to the accuracy of measured patterns. Nevertheless, "little difference" could amount to 1 dB or more of error in measurement of sidelobe power at levels below about 25 dB with respect to peak main lobe gain. Often the right hand side of the above far field equation is modified to $\frac{4D^2}{\lambda}$ for improved results.

These simple formulae drive the required measurement distance for a far field measurement range. For distances of about 2–3 m anechoic chambers are quite practical and, relative to larger measurement ranges, quite low in cost. Many such small chambers are to be found in university research groups and commercial organizations. Often, either a single axis positioner (rotator) will be used to facilitate measurement of principle planes, or two-axis (e.g., elevation over azimuth positioners are used.)

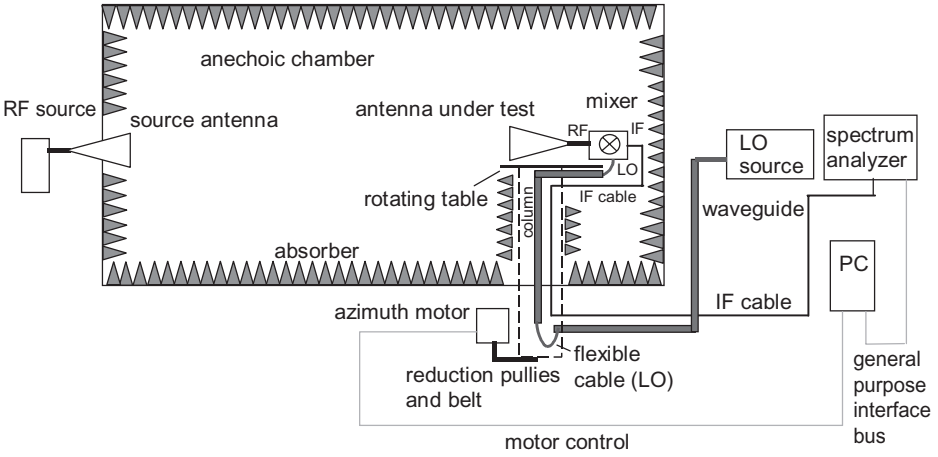

Figure 1.28. A single axis antenna pattern measurement system.

A relatively simple antenna measurement system is illustrated in Figure 1.28.

In Figure 1.28 the system is configured to measure power only—the spectrum analyzer is being used as a power meter. A motor drives a turntable in azimuth hence the AUT, the table to which it is mounted and the supporting column are rigidly connected. A computer (PC) commands the turntable motor in discrete angular increments and for each of these the received power is recorder, thus capturing a table of results with two columns: power vs. angle. The chamber is lined with absorbing material, typically a type of carbon-loaded foam of pyramidal shape (Fig. 1.29). The lengths of these pyramidal blocks influences the frequency range over which the absorber is effective. Shorter lengths (a few cm) with fine points are best for several GHz upwards, while longer lengths (a few 10s of cm) better for around 1 or 2 GHz. At lower frequencies the pyramidal points can be truncated if their shortest dimension is somewhat less than a wavelength. Any structures inside the chamber, for example, the turntable/column housing, should be similarly screened such as the rotating column inside the tower structure in Figure 1.30.

Various approaches to signal routing can be chosen depending on available equipment and budget. In Figure 1.28 a system is illustrated where the power measurement is made at an intermediate frequency. This offers the advantage of very much reduced loss in the cable between the AUT and the power detector (spectrum analyzer). Of course, some other type of power meter could also be used. In contrast, a measurement of power at the RF frequency would tend to lead to a much more lossy circuit between AUT and detector, and require a more costly detector. On the other hand, a disadvantage of measuring at IF is the need to down convert the RF signal. In Figure 1.28 this entails use of a mixer and local oscillator (LO). A good cost compromise, shown here, is using a harmonic mixer which is driven at around half the RF frequency. To take an example, for an RF frequency of 30 GHz the LO could be around 14.5 GHz to produce an IF at

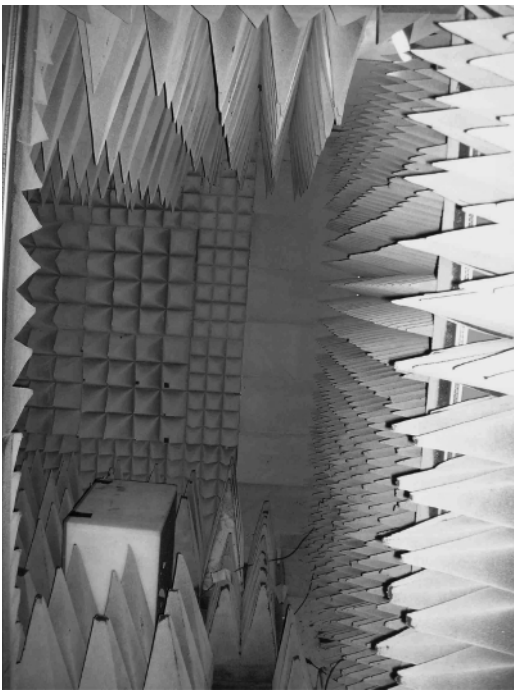

Figure 1.29. View of an anechoic chamber interior (photo: J. Thornton).

1 GHz. An important property of the mixer includes the required LO input power, which in turn influences the loss which can be tolerated in the LO circuit. If the mixer is a biased type (where direct current bias is applied to the mixer diodes) the LO power requirement is reduced. For non-biased mixers operating at the second harmonic, around + 10 dBm of LO power might be needed. The circuit between LO source and mixer might exhibit many dB of attenuation, but this can be minimized by substituting waveguide for cable as far as practically possible: this is indicated in Figure 1.28 where cable is only used for the rotating interface and the interconnections at the mixer and source. Another measure to ensure adequate LO power would be use of an amplifier (mixers can also be obtained with integrated LO amplifiers) so that loss in the LO circuit can be better tolerated.

All sorts of alternative configurations to that illustrated in Figure 1.28 would be practicable. The two sources (signal generators) could be replaced with a single item and power divided between RF and LO duties, implying of course that both are at the same frequency and so the mixer operates in the fundamental mode (not harmonic). Coherence of these two signals also implies a homodyne detection system and so one that is highly sensitive to the path length between source antenna and AUT and hence to any misalignment of the AUT phase center from the axis of rotation. Other laboratory configurations use a vector network analyzer effectively to perform both source and

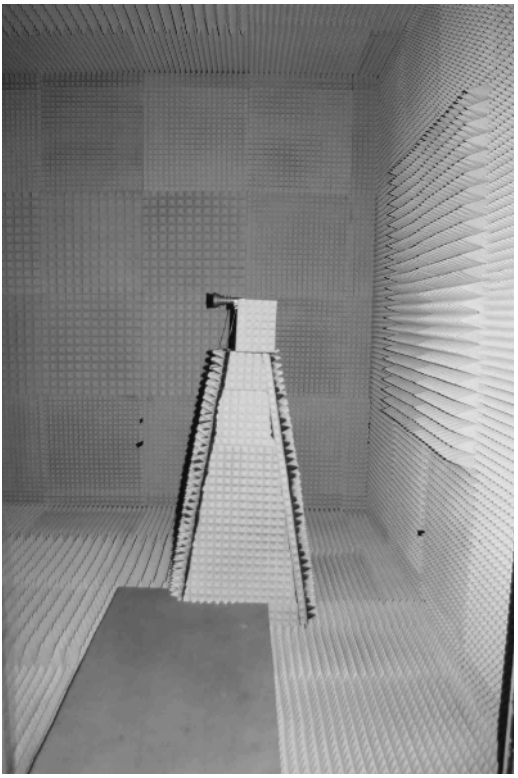

Figure 1.30. Column in anechoic chamber screened by absorber (photo: J. Thornton.)

receiver functions and with the additional benefit of phase measurements should such be required.

Too small a chamber will prove restrictive for many electrically large antennas where longer distances are imposed by the far field condition. Some large organizations have constructed anechoic chambers on much larger scales, such as the European Space Agency's $12.5 \times 8.5 \times 4.5$ m range at their European Space Research and Technology Centre (ESTEC) facility in The Netherlands (see photograph of Fig. 1.31). This chamber however is configured as a Compact Antenna Test Range (CATR), where far field conditions are brought about by use of a shaped reflector which yields a plane wave (or "quiet") zone in the proximity of the antenna under test. This reflector is seen on the right hand side of the image in Figure 1.31 and it is illuminated by an antenna on the balcony seen just left of center. The quiet zone where the positioner and AUT is placed is in the region on the very far left.

ESA's chamber is sufficiently large to contain entire satellites or payloads for analysis of payload antenna patterns, and for these purposes a multi-axis positioner is also installed. The CATR principle is also used in smaller chambers.

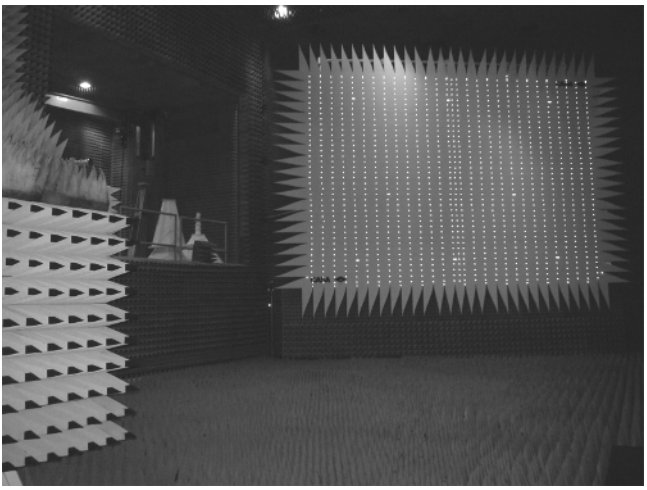

Figure 1.31. ESA's indoor compact range. (photo: J.Thornton).

For true far field measurement at longer ranges outdoor sites are used. Here, the principle of operation is conceptually the most straightforward, but the main issues are how to suppress or otherwise account for ground reflections, outside electromagnetic interference, and effects of the weather (either in terms of electrical attenuation and scattering, or environmental protection of equipment).

In contrast to far field or CATR methods, near field measurements are the other family of methods used for antenna pattern measurements and these are also well suited to indoor installation. Here the far field is not measured directly but derived from data gathered over a surface in the radiating near field (*Fresnel*) zone of the antenna under test (AUT). The surfaces most often encountered are spherical, cylindrical or planar. In each case the surface relates to both the mathematical transform used to derive far field results from near field data, and the mechanical properties of the scanning system. The data are derived as a set of two-port measurements where phase and amplitude are recorded for the transmission path between transmit and receive ports. In some cases the AUT is physically moved or rotated, or a probe in the measurement plane is moved, or combinations can occur.

Figure 1.32 illustrates the geometry of a typical spherical near field scanner. Here, either antenna may be the transmitter or receiver but most often the AUT is the receiver, as illustrated. The AUT is mounted on a mechanical two-axis rotator. One axis (e.g., θ) is first set, then the second (e.g., ϕ) swept through a circle and data recorded at fixed angular increments. The first angle is then incremented and the second swept through the full range. The order does not greatly matter, but determines whether data is captured around a set of circles resembling lines of latitude (Fig. 1.33a) or lines of longitude (Fig. 1.33b).

The equipment in the left hand and right hand sides in Figure 1.32 (i.e., the two antennas) may be located at opposite ends of a laboratory or chamber, or they

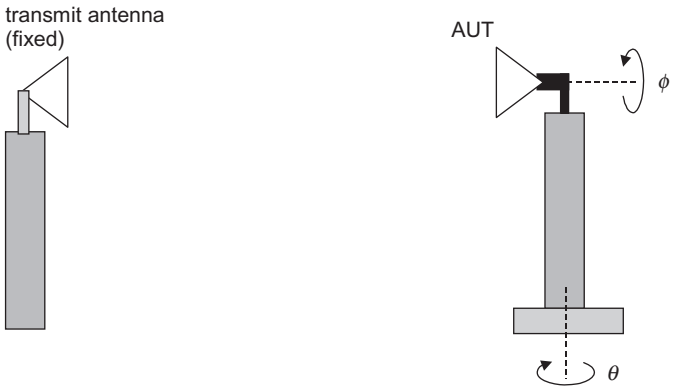

Figure 1.32. Spherical near field scan measurement.

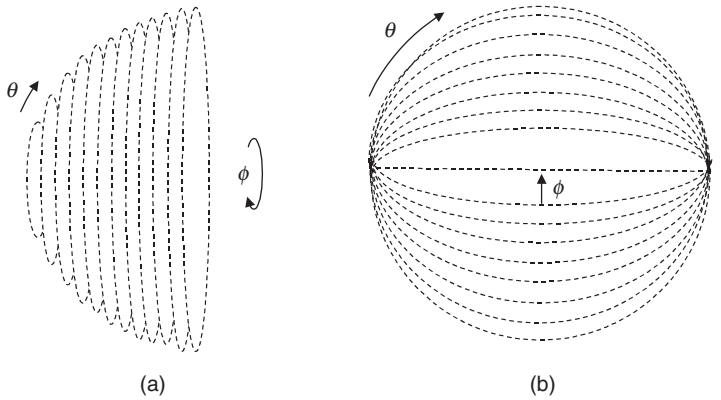

Figure 1.33. Spherical scans: (a) θ then ϕ, (b) ϕ then θ.

may be rigidly linked on a single piece of bench equipment such as that illustrated in Figure 1.34.

A variant of the near field class of methods is the "scalar only" near field type. Here, scalar data (amplitude only) is recorded over two surfaces at a fixed separation, for example over two planes which are a few wavelengths apart. While a single plane of scalar sampled near field data does not contain sufficient information to derive the far field, it is possible to infer the missing phase data where a second plane of scalar data is available. The process is iterative whereby the scalar data is successively transformed between planes, overwritten, and transformed again repeatedly so that the phase data "grows" in the matrix of samples. The method is considered analogous to holography. Convergence can be slow, but speeded up if other boundary conditions are invoked such as the truncation of the physical radiating aperture. The advantage is that

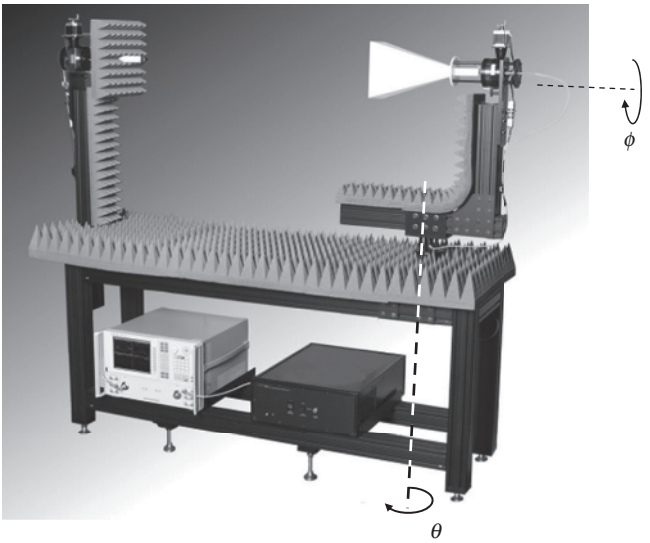

Figure 1.34. A near field spherical axis scanner (image courtesy of Nearfield Systems Inc, Torrance, CA, USA.)

the instruments used tend to be somewhat less costly since only a scalar detector is required.

Each of these three main categories also have different strengths and weaknesses, or areas of applicability. For example, the spherical method samples all the radiated field around an antenna and so can derive its far field pattern in all of space. As such, for mechanical reasons it is well suited for the measurement of smaller antennas, and for electrical reasons it is well suited to broad or quasi-omnidirectional patterns. Of course, these two properties (small/electrically small antenna and low directivity) tend to coincide. In contrast, the planar method samples data across a planar, usually rectangular zone close to the radiating aperture. As such, it can at best only derive far field pattern in one half of space, but in practice in an angular region somewhat less than this because of the finite extent of the spatial sampled area. It is well suited to electrically large and highly directional antennas. A very comprehensive treatise on planar near field measurements is found in Reference 61, while further details of far-field and near-field measurements in general can be found in Reference 62.

REFERENCES

[1] D. L. Sengupta and T. K. Sarkar, "Microwave and Millimeter Wave Research before 1900 and the Centenary of the Horn Antenna," Microwave Conference, 1995. 25th European, Vol. 2, pp. 903–909, 1995.

[2] F. G. Friedlander, "A dielectric-lens aerial for wide-angle beam scanning," IEE Electrical Engineers—Part IIIA: Radiolocation, pp. 658–662, 1946.

[3] K. Khoury and G. W. Heane, "High performance lens horn antennas for the millimeter bands," IEE Colloquium on Radiocommunications in the Range 30–60 GHz, 10/1–10/9, 1991.

[4] B. S. Westcott and F. Brickell, "General Dielectric-Lens Shaping Using Complex Co-ordinates," IEE Proceedings, Part H—Microwaves, Antennas and Propagation, Vol. 133, pt. H, no. 2, p. 122–126, April 1986.

[5] C. A. Fernandese, P. O. Frances, and A. M. Barbosa, "Shaped Coverage of Elongated Cells at Millimetrewaves Using a Dielectric Lens Antennas," Microwave Conference, 1995. 25th European, pp. 66–70, 1995.

[6] A. D. Olver and B. Philips, "Integrated Lens with Dielectric Horn Antenna," Electron. Lett. Vol. 39, 1993, pp. 1150–1152.

[7] N. G. Ugras, J. Zmuidzinas, and H. G. LeDuc, "Quasioptical SIS Mixer with a Silicon Lens for Submillimeter Astronomy," in Proceedings of 5th International Symposium Space Terahertz Technology, p. 125, 1994.

[8] J. W. Lamb, "Miscellaneous Data on Materials for Millimeter and Submillimeter Optics," Int. J. Inf. Millim. Waves Vol. 17, No. 12, 1996, pp. 1997–2034.

[9] C. R. Englert, M. Birk, and H. Maurer, "Antireflection Coated, Wedged, Single Crystal Silicon Aircraft Window for the Far-Infrared," IEEE Trans. Geosci. Remote Sens. Vol. 37, July 1999, pp. 1997–2003.

[10] A. J. Gatesman, J. Waldman, M. Ji, C. Musante, and S. Yngvesson, "An Anti-Reflection Coating for Silicon Optics at Terahertz Frequencies," IEEE Microw. Guid. Wave Lett. Vol. 10, No. 7, 2000, pp. 264–267.

[11] Dielectric Chart, Emerson & Cuming Microwave products, MA, 2010.

[12] H. Mosallaei and Y. Rahmat-Samii, "Nonuniform Luneburg and Two-Shell Lens Antennas: Radiation Characteristic Sand Design Optimization," IEEE Trans. Antennas Propag. Vol. 49, No. 1, January 2001, pp. 60–69.

[13] T. Komljenovic, R. Sauleau, and Z. Sipus, "Synthesizing Layered Dielectric Cylindrical Lens Antennas," APS Symposium, San Diego, July 2008.

[14] D. S. Weileand and E. Michielssen, "Genetic Algorithm Optimization Applied to Electromagnetics," IEEE Trans. Antennas Propag. Vol. 45, No. 3, March 1997, pp. 343–353.

[15] J. Robinson and Y. Rahmat-Samii, "Particle Swarm Optimization in Electromagnetics," IEEE Trans. Antennas Propag. Vol. 52, No. 2, February 2004, pp. 397–407.

[16] R. Sauleau and B. Barés, "A Complete Procedure for the Design and Optimization of Arbitrarily Shaped Integrated Lens Antennas," IEEE Trans. Antennas Propag. Vol. 54, No. 4, 2006, pp. 1122–1133.

[17] C. A. Balanis, Antenna Theory: Analysis and Design, 3rd ed., Wiley-Interscience, Hoboken, NJ, 2005.

[18] A. D. Olver, P. J. B. Clarricoats, A. A. Kishk, and L. Shafai, Microwave Horns and Feeds, IEEE Press, New York, 1994.

[19] C. Salema, C. Fernandes, and R. K. Jha, Solid Dielectric Horn Antennas, Artech House, Norwood, 1998.

[20] A. D. Olver and A. A. Saleeb, "Lens-Type Compact Antennas Range," Electron. Lett. Vol. 15, No. 14, 1979, pp. 409–410.

[21] S. Bishay, S. Cornbleet, and J. Hilton, "Lens Antennas with Amplitude Shaping or Sine Condition," Proc. IEE Vol. 136, No. 3, 1989, pp. 276–279.

[22] C. J. Sletten, Reflector and Lens Antennas—Analysis and Design Using Personal Computers, Artech House, Norwood, 1988.

[23] C. Fernandes, M. Filips, and L. Anunciada, "Lens Antennas for the SAMBA Mobile Terminal," Proceedings of the ACTS Mobile Telecommunications Summit 97, Aalborg, Denmark, pp. 563–568, 1997.

[24] R. K. Luneberg, United States Patent 2,328,157, Issue Date: August 31, 1943.

[25] M. Rayner, Use of Luneburg lens for low profile applications", Datron/Transco Inc. Microw. Product Dig., December 1999.

[26] X. Wu and J. J. Lauren, "Fan-Beam Millimeter-Wave Antenna Design Based on the Cylindrical Luneberg Lens," IEEE Trans. Antennas Propag. Vol. 55, No. 8, 2007, pp. 2147–2156.

[27] E. G. Zelkin and R. A. Petrova, Lens Antennas, Sovetskoe Radio Publ., Moscow, (in Russian), 1974.

[28] J. Fox, Proceedings of the Symposium on Quasi-Optics, Polytechnic Press, Brooklyn, NY, 1964.

[29] P. F. Goldsmith, "Quasioptical Techniques," Proc. IEEE Vol. 80, No. 11, 1992, pp. 1729–1747.

[30] J. C. G. Lesurf, Millimeter- Wave Optics, Devices, and Systems, Adam Hilger, Bristol, 1990.

[31] O. J. Lodge and J. L. Howard, "On Electric Radiation and its Concentration by Lenses," Proc. Physical Soc. Lond. Vol. 10, No. 1, 1888, pp. 143–163.

[32] E. Karplus, "Communication with quasioptical waves," Proc. IRE Vol. 19, October 1931, pp. 1715–1730.

[33] F. Sobel, F. L. Wentworth, and J. C. Wiltse, "Quasi-Optical Surface Waveguide and Other Components for the 100 to 300 Gc Region," IEEE Trans. Microw. Theory Tech. Vol. MlT-9, No. 6, 1961, pp. 512–518.

[34] E. Wolf, "Microwave Optics," Nature Vol. 172, 1953, pp. 615–616.

[35] H. Kosaka, T. Kawashlma, A. Tomita, M. Notami, T. Tomamura, T. Sato, and S. Kawakami, "Superprism Phenomena in Photonic Crystals: Toward Microscale Lightwave Circuits," J. Lightwuve Technol. Vol. 17, No. 11, 1999, pp. 2032–2038.

[36] J. B. Pendry, "Negative Refraction Index Makes a Perfect Lens," Phys. Rev. Lett. Vol. 85, 2000, pp. 3966–3969.

[37] J. Volakis, Antenna Engineering Handbook, 4th ed., McGraw-Hill Professional, New York, June 2007.

[38] A. Petosa and A. Ittipiboon, "Shadow Blockage Effects on the Aperture Efficiency of Dielectric Fresnel Lenses," IEE Proc.-Microw. Antennas Propag. Vol. 147, No. 6, December 2000, pp. 451–454.

[39] B.-I. Wu, W. Wang, J. Pacheco, X. Chen, T. Grzegorczyk, and J. A. Kong, "A Study of Using Metamaterials as Antenna Substrate to Enhance Gain," PIER Vol. 51, 295–328, 2005, pp. 295–329.

[40] D. R. Smith, W. J. Padilla, D. C. Vier, S. C. Nemat-Nasser, and S. Schultz, "Composite Medium with Simultaneously Negative Permeability and Permittivity," Phys. Rev. Lett. Vol. 84, No. 18, May 2000, pp. 4184–4187.

[41] D. Staiculescu, N. Bushyager, and M. Tentzeris, "Microwave/ Millimeter Wave Metamaterial Development Using the Design of Experiments Technique," IEEE Applied Computational Electromagnetics Conference, pp. 417–420, April 2005.

[42] E. Ozbay, K. Aydin, E. Cubukcu, and M. Bayindir, "Transmission and Reflection Properties of Composite Double Negative Metamaterials in Free Space," IEEE Trans. Antennas Propag. Vol. 51, No. 10, October 2003, pp. 2592–2595.

[43] R. A. Shelby, D. R. Smith, and S. Schultz, "Experimental Verification of a Negative Index of Refraction," Science Vol. 292, April 2001, pp. 77–79.

[44] G. V. Eleftheriades, A. K. Iyer, and P. C. Kremer, "Planar Negative Refractive Index Media Using Periodically L-C Loaded Transmission Lines," IEEE Trans. Microw. Theory Tech. Vol. 50, No. 12, December 2002, pp. 2702–2712.

[45] A. Grbic and G. V. Eleftheriades, "Experimental Verification of Backward-Wave Radiation from a Negative Refractive Index Material," J. Appl. Phys. Vol. 92, No. 10, November 2002, pp. 5930–5935.

[46] C. Caloz and T. Itoh, "Novel Microwave Devices and Structures Based on the Transmission Line Approach of Meta-Materials," IEEE MTT-S Digest, pp. 195–198, 2003.

[47] C. Metz, "Phased Array Metamaterial Antenna System," US Patent US2005225492 (A1) Issued on October 25, 2005.

[48] T. Ueda, A. Lai, and T. Itoh, "Negative Refraction in a Cut-off Parallel-Plate Waveguide Loaded with Two-Dimensional Lattice of Dielectric Resonators," 36th European Microwave Conference, pp.435–438, Manchester, U.K., September 2006.

[49] S. Kamada, N. Michishita, and Y. Yamada, "Metamaterial Lens Antenna Using Dielectric Resonators for Wide Angle Beam Scanning," IEEE Antennas and Propagation Society International Symposium (APSURSI), pp. 1–4, 2010.

[50] D. M. Pozar, "Flat Lens Antenna Concept Using Aperture Coupled Microstrip Patches," Electron. Lett. Vol. 32, No. 23, November 1996, pp. 2109–2111.

[51] M. R. Chaharmir, J. Shaker, M. Cuhaci, and A. Sebak, "Mechanically Controlled Reflectarray Antenna for Beam Switching and Beam Shaping in Millimeter Wave Applications," Electron. Lett. Vol. 39, No. 7, 2003, pp. 591–592.

[52] J. Huang and A. Feria, "A One-Meter X-band Inflatable Reflectarray Antenna," Microw. Opt. Technol. Lett. Vol. 20, January 1999, pp. 97–99.

[53] J. Huang and A. Feria, "Inflatable Microstrip Reflectarray Antennas at X and Ka-band Frequencies," IEEE AP-S, Orlando, Florida, pp. 1670–1673, July 1999.

[54] J. Thornton and D. J. Edwards, "Modulating Retroreflector as a Passive Radar Transponder," Electron. Lett. Vol. 34, No. 19, September 1998, pp. 1880–1884.

[55] B. A. Munk, Frequency Selective Surfaces: Theory and Design, John Wiley and Sons Inc., New York, 2000.

[56] N. Gagnon, A. Petosa, and D. A. McNamara, "Thin Microwave Quasi-Transparent Phase-Shifting Surface (PSS)," IEEE Trans. Antennas Propag. Vol. 58, No. 4, April 2010, pp. 1193–1201.

[57] A. Abbaspour-Tamijani, K. Saranbandi, and G. M. Rebeiz, "A Millimeter-Wave Bandpass Filter-Lens Array," IET Microw. Antennas Propag. Vol. 1, No. 2, April 2007, pp. 388–395.

[58] J. C. Wiltse, "Fresnel Zone-Plate Lenses," Proceedings of SPIE, Vol. 544, Millimeter-Wave Technology III, July 1985.

[59] H. D. Hristov, Fresnel Zones in Wireless Links, Zone Plate Lenses and Antennas, Artech House, Norwood, MA, 2000.

[60] N. Gagnon, A. Petosa, and D. A. McNamara, "Comparison between Conventional Lenses and an Electrically Thin Lens Made Using a Phase Shifting Surface (PSS) at Ka Band,"

Loughborough Antennas & Propagation Conference, pp.117–120, 16–17 November 2009, Loughborough, UK.

[61] S. Gregson, J. McCormick, and C. Parini, Principles of Planar Near-Field Antenna Measurements, IET Electromagnetic Wave Series 53, The Institute of Engineering and Technology, London, 2007.

[62] G. Evans, Antenna Measurement Techniques, Artech House, Norwood, MA, 1990.